Flood risk assessment using GIS and multi-criteria analysis: a pilot study from Rönne å River basin, Scania, Sweden

Florian Steichen

2024
Department of
Physical Geography and Ecosystem Science
Lund University
Sölvegatan 12
S-223 62 Lund
Sweden

Florian Steichen (2024).
Title of thesis (Flood risk assessment using GIS and multi-criteria analysis: a pilot study from Rönne å River basin, Scania, Sweden)
Bachelor degree thesis, 15 credits in Physical Geography and Ecosystem Analysis
Department of Physical Geography and Ecosystem Science, Lund University

Level: Bachelor of Science (BSc)

Course duration: *January* 2024 until *June* 2024

Disclaimer

This document describes work undertaken as part of a program of study at the University of Lund. All views and opinions expressed herein remain the sole responsibility of the author, and do not necessarily represent those of the institute.

Flood risk assessment using GIS and multi-criteria analysis: a pilot study from Rönne å River basin, Scania, Sweden

Florian Steichen

Bachelor thesis, 15 credits, in Physical Geography and Ecosystem Analysis

Supervisor 1 Karin Larsson
Affiliation

Supervisor 2 name
Affiliation

Exam committee:
Examiner 1, Affiliation
Examiner 2, Affiliation

<u>Acknowledgements</u>

First and foremost, I would like to thank my supervisor, Karin Larsson, for her constant support throughout my thesis and for guiding me in the right direction when things felt uncertain. I also want to thank David McGauran for always being there for me in stressful moments and going over my thesis way too many times. Lastly, I am very grateful to Amber Keating Foley for keeping me on track with my progress and for providing the initial ideas that shaped my thesis.

Abstract

Following the flooding event in Ringsjön within the Rönne å river basin in January 2024, this catchment area was utilized for a flood risk assessment. The study focused on the precipitation event during August 2023, known as Storm Hans. The flood risk assessment for the Rönne å catchment area was conducted using multi-criteria analysis (MCA) and geographical information systems (GIS). Seven factors impacting flooding were considered in the MCA: slope, elevation, monthly precipitation, land use, soil texture, proximity to water bodies, and drainage density, based on the studies by Noori & Bonakdari (2023), Ali et al. (2023), and Hagos et al. (2022). The factors were ranked according to the weights provided in these three studies, as well as one analysis assigning equal weights to all factors. The factors were normalized using fuzzy linear equations, resulting in values that ranged from 0 (very low flood risk) to 1 (very high flood risk). These normalized factors were combined using the weighted linear combination (WLC) method to create four distinct flood risk maps, where each map was based on the different weights used in the articles. The reliability of these maps was evaluated by overlaying them with a flood map created by Sweco, which utilized the hydraulic model MIKE 11. Since MIKE 11 is a flood simulation model, the resulting polygon from this analysis was considered to represent a 100% very high flood risk. Consequently, when the different maps from the MCA were overlaid with this polygon, the higher the percentage of the high-risk class in that area, the more reliable the map was assumed to be. The map based on the weights from Hagos et al. (2022) proved to be the most accurate, where 79% of the overlaid area with the MIKE 11 model was classified as high and very high risk. Conversely, the map using weights from Noori & Bonakdari (2023) was the least accurate, where only 29% of high to very high areas were found in the polygon layer produced by Sweco.

Key Words: GIS, MCA, Rönne å, flood risk assessment, fuzzy membership, WCL, extreme precipitation, climate change

Table of Contents

1 Introduction and Background

1.1 Background

Inland flooding

In an era increasingly shaped by global climate change, it is crucial to monitor and understand its impacts. Among its effects, inland flooding stands out for its increased frequency and intensity which poses significant challenges (Earth Networks, 2023). Inland floods are characterized by the accumulation of water on typically dry land and can broadly be classified into fluvial and pluvial flooding (Earth Networks, 2023). On the one hand, fluvial floods occur when water levels in rivers exceed their banks or when man-made dikes are breached. On the other hand, pluvial floods occur after intense rainfall events, where the ground's capacity to absorb water is surpassed and consequently leads to surface runoff (Thieken et al., 2022). The underlying cause of inland flooding is predominantly rainfall, which can fall as either intense, short-duration precipitation or as prolonged, steady rainfall over several days or weeks (Earth Networks, 2023). These precipitation events can significantly elevate flood risks, especially when combined with pre-existing conditions like saturated soils or rapid snowmelt (Thieken et al., 2022). The impact of global warming intensifies these conditions. Increased temperatures lead to higher evaporation rates and an increased capacity of the atmosphere to hold moisture, which creates conditions for more severe and prolonged rainfall (United Nations Environment Programme, 2020).

Flooding in the Rönne å catchment

The recent flooding event that happened in January 2024 in the Rönne å catchment, especially around lake Ringsjön illustrates the implications of these intense weather events. In the fall of 2023, an unusually heavy rainfall due to the storm Hans led to saturating the soil in the Rönne å catchment area which resulted in exceptionally high-water levels in Rönne å downstream. This prevented the Ringsjön lake from draining efficiently into the river, which is the source of the Rönne å river (Tan & Gullmander, 2024; Nordström, 2024). A shift to milder weather across Sweden during the end of January caused rapid snowmelt that had fallen over the winter in southern Sweden. This worsened the situation as the already saturated soils increased flow rates in the region's waterways, which eventually led to flooding of Ringsjön and its surrounding areas (SMHI, 2024 ; Nordström, 2024). This flood event that occurred in January is not out of the ordinary for the Rönne å catchment. The Rönne å catchment area has experienced regular flooding in previous years (Kalimukwa & Mohamed, 2021). Studies have shown that there have been other significant high flows in the Rönne å catchment, indicating high flood risks

(Kalimukwa & Mohamed, 2021). This highlights the importance of continuous monitoring and assessment of flooding to better understand and manage flood risks in the Rönne å catchment.

History of Land use Change in Skåne and its effect on flooding

The historical land use changes in Skåne, especially the drainage of wetlands, have significantly increased its susceptibility to flooding (Krug, 1993). The widespread drainage of wetlands was driven by rapid population growth and the need for more agricultural land, where approximately 100 km² of wetlands were drained, and about 1160 km of streams were affected through channelization or covered drainage (Krug, 1993). When wetlands are drained or removed, the land loses the ability to absorb and store excess water. This leads to increased surface runoff, and consequently more severe flooding downstream (Department of Environmental Conservation, 2024). Furthermore, man made dikes accelerate the natural flow which makes it harder to control the water level and gives less time for the soil to absorb water which also increases the risk of flooding as well (Sofia & Tarolli, 2017).

Climate Change in Sweden and its effect on flooding

Moreover, Sweden is experiencing significant climatic shifts, where an increase in extreme precipitation events is anticipated throughout Sweden (Eklund et al., 2015). The most significant changes are expected during the winter months, along with an overall increase in annual rainfall for most of the country (Eklund et al., 2015). These shifts in precipitation patterns are associated with the expected future increased greenhouse gas concentrations, particularly under the representative concentration pathway (RCP8.5) scenario, which hints towards intensified hydrological impacts. Recent analyses suggest that Sweden may experience more severe extreme flows than previously estimated, based on outcomes from nine global climate models and scenarios RCP4.5 and RCP8.5 (Eklund et al., 2015). Consequently, these climatic shifts, especially in precipitation patterns, are indicating that flooding events are expected to become more frequent and severe in Sweden (Eklund et al., 2015).

Multi-Criteria-Analysis and its importance on flood risk mapping

The GIS-based multi-criteria analysis (MCA) is increasingly used for flood risk assessment due to its efficiency and cost-effectiveness compared to traditional hydrological and hydraulic models such as Mike11. The MCA method utilizes available spatial and demographic data to evaluate flood risk, making it particularly suitable for regions with limited resources (Rincón et al., 2018). A significant advantage of MCA, especially when integrated with the Analytic Hierarchy Process (AHP), is its capability to assign weights to various criteria through pairwise comparisons. This approach ensures that the assessment reflects the relative importance of all relevant factors (Malczewski & Rinner, 2015). Furthermore, thanks to the flexibility of the methodology of the MCA, it is possible to include new criteria and adjust weights as more data becomes available which makes the model adaptable to changing environmental and

developmental conditions (Malczewski, 1999; Malczewski & Rinner, 2015). In this paper, the methodology incorporates various factors, including slope, elevation, precipitation patterns, land use, soil texture, proximity to water bodies, and drainage density as proposed by Ali et al. (2023), Noori & Bonakdari (2023) and Hagos et al (2022).

Importance of flood risk mapping and mitigation strategies

The projected increase in precipitation and extreme weather events due to climate change necessitates a thorough understanding and preparation for inland flooding. Implementing effective flood risk management strategies is crucial to mitigate the impacts on communities, infrastructure, and ecosystems. Through an analysis of risk factors and the identification of vulnerable areas, it is possible to implement measures that improve resilience and reduce the potential for damage. Adaptation strategies for flood risk management may include the restoration of natural floodplains, the implementation of green infrastructure solutions such as rain gardens and permeable pavements, and the development of early warning systems (SerraLlobet et al., 2022). These strategies can increase the natural capacity of the landscape to store water, reduce runoff, and provide time for communities to prepare for floods.

1.2 Study area

The study was carried out in the Rönne å river basin in the south of Sweden which is presented in figure 1.
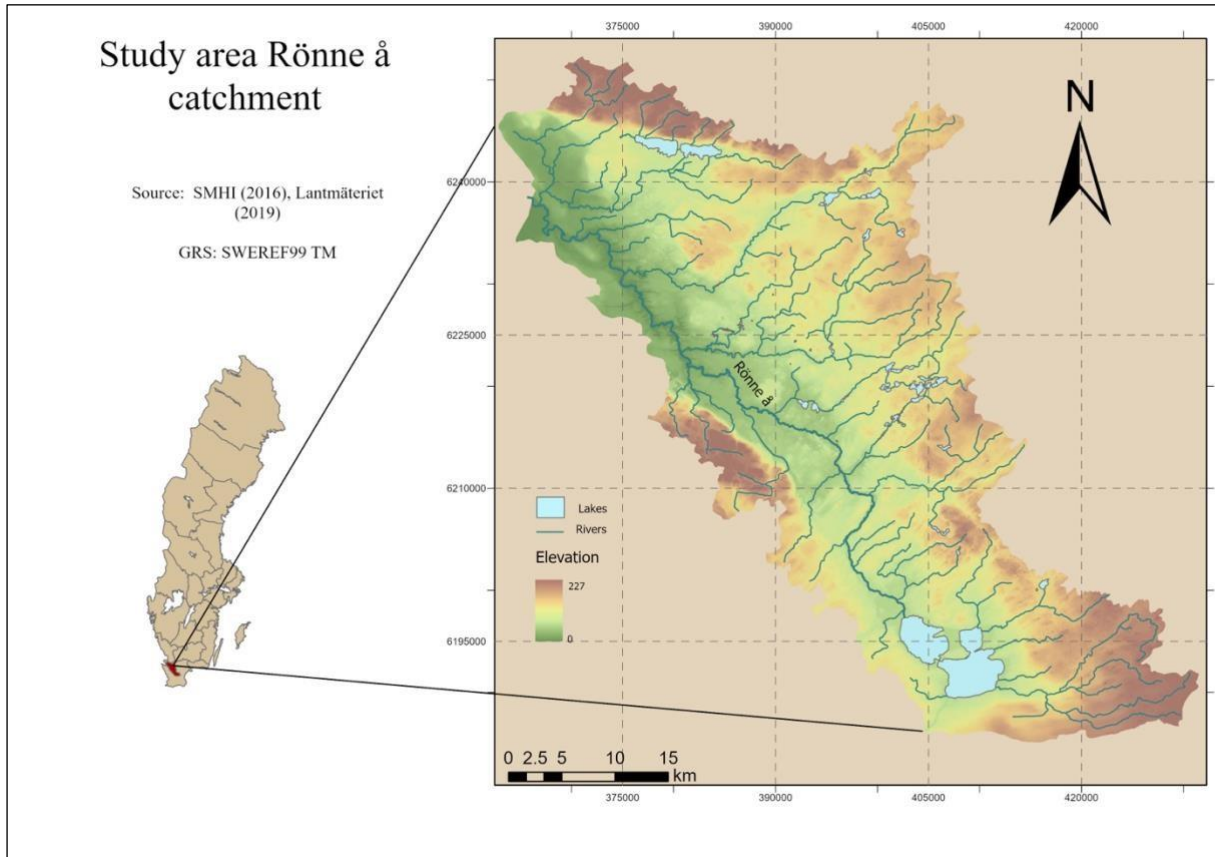
Figure 1: Study area of Rönne å with major waterbody and elevation

The catchment of Rönne å river has an area of 1897 km^2 with an annual precipitation of 700 mm (Inamdeen et al., 2021). It is predominated by forest, agricultural land, wetland, and lakes with some settlement areas, which constitute around 88% of the land use in the Rönne catchment area (Inamdeen et al., 2021). The main soil types in the Rönne catchment are Loamy sand with 73% and loam which constitutes 18% of the river basin (Kronvang et al., 2005). The catchment has a diverse topography, ranging from flat and low coastal plains near the Kattegat Sea to a more hilly relief further inland (Lidmar-Bergström et al., 1991). It reaches from around sea level to around 220 m above sea level (Läntmateriet, 2019). The catchment area presents a range of landforms, which are primarily shaped by glacial activity during the last Ice Age (Lidmar-Bergström et al., 1991). Glaciers shape landscapes through erosional and depositional processes which forms distinctive features such as moraines and outwash plains (Lidmar-Bergström et al., 1991). Moraines are formed from glacial debris that accumulates at

the edges of glaciers, creating ridges that can vary in size and consist of a mixture of rocks, soil, and other materials. In contrast, outwash plains are formed by meltwater flowing from glaciers, which deposits sediment in well-sorted layers (Bennett & Glasser, 2009). The most common landforms and key features within the Rönne å catchment area are water gaps formed by glaciers, drumlins and transverse moraine ridges (Lidmar-Bergström et al., 1991).

The majority of the bedrock in southwest Scania was formed during the Paleozoic era and consists of reef limestone, shale, alun shale, sandstone and conglomerate (Fransson et al., 2004). The Romele horst is one of several crystalline horsts in Scania, located just northeast along the Tornquist zone. The western fault and folding zone of the horst is the largest in this region (Erlström, 2009). Periodic tectonic activity in the strata has, in some cases, caused layer inversion, placing older layers atop younger ones (Erlström, 2009). These tectonic activities have led to uplift along the horst and tilting of the bedrock toward the southwest. The uplift has facilitated sedimentation and erosion, resulting in the deposition of Cambrian and Silurian rocks (Erlström, 2009).

1.3 Aim and hypothesis

Aim

This paper aims to identify areas within the Rönne å catchment that are most susceptible to flooding using the MCA methodology proposed by Ali et al. (2023), Noori & Bonakdari (2023) and Hagos et al. (2022). By doing so, the study will produce four different flood risk maps, three based on weights from each of the three articles and one based on equally weighted factors, thereby highlighting vulnerable zones. The analysis will focus on the following factors: slope, elevation, proximity to river, drainage density, soil texture, and land cover. Additionally, the study will assess if these factors and weights are appropriate for the specific climatic and geographic conditions of the Rönne å catchment by comparing the results with the map from Sweco (2014) which uses the hydraulic model MIKE 11. The accuracy of the MCA will be tested by overlaying the produced maps with the Sweco map to identify overlapping areas. It is important to note that the produced flood risk maps will only account for relative spatial variation in flood risk and will not consider temporal factors such as pre-existing conditions, soil moisture, or groundwater levels that influence flooding.

Key Objectives

- Develop flood risk maps for the Rönne å catchment based on monthly precipitation from August 2023.
- Identify regions particularly vulnerable to flooding events.
- Examine the accuracy of the MCA by comparing it with the flood map from Sweco.
  - Compare different flood-risk models through visual comparison.
  - Quantify areas of differences and discuss limitations.
- Analyze monthly metrological precipitation data over the Rönne catchment from 2023 to assess if it can be classified as an extreme precipitation event.

Hypotheses

- The flood risk maps produced by the MCA will show similar patterns of high risk compared to the hydrodynamic model MIKE 11 from Sweco (2024).
- Areas close to rivers and lakes will be most affected by flooding.
- The month of August 2023 has been a month that can be classified as an extreme precipitation event.

2 Material and Methods

2.1 Material

The following data was selected for the MCA:

Table 1: Datasets and corresponding metadata selected for multi-criteria model factors.

Dataset	Variable	Source	Resolution	Geographic Reference	Notes
DEM	Elevation (m)	Läntmateriet (2019)	2 m	SWEREF 99	(version 1.4)
Precipitation	monthly rainfall (mm)	SMHI (2024)	4000m	SWEREF 99	Gridded precipitation data
Soil Type	Soil	SGU (2018)	/	SWEREF 99	Vector Format
Land use	Land use type	NMD (2018)	10m	SWEREF 99	Raster Format
River network	Rönne å	SMHI (2016), Läntmateriet (2016)	/	SWEREF 99	Vector Format
Water bodies	Lakes	NMD (2018)	10m	SWEREF 99	Raster Format
Catchment	Rönne å catchment	SMHI (2016)	/	SWEREF 99	Vector Format
MIKE 11 model	200-Year river flow	SWECO (2014)	/	SWEREFF 99	Vector Format
Average precipitation	Monthly rainfall (mm)	SMHI (2024)	/	SWEREFF 99	Meteorologic measurement data from Hörby A station

2.2 Methods

2.2.1 Extreme precipitation

Extreme precipitation describes the scenario during which the amount of rain or snowfall experienced in a location significantly exceeds the norm. Statistically, it can be defined as precipitation that exceeds the usual range by two or more standard deviations (std.) above the mean for a particular area during a specific period (EPA, 2023). Storm Hans occurred in early August 2023 and significantly impacted Sweden's precipitation patterns. On August 8th, it brought some of the heaviest rainfall, exceeding 80 mm per day, and persisted for several days, which caused extensive flooding and damage (Messori & Faranda, 2023). This storm was unusually powerful for the season and led to higher-than-usual precipitation levels across Scandinavia (Messori & Faranda, 2023). To confirm that the month of August (2023) deviated from the mean in the Rönne å catchment area, the average mean for the month of August was computed from the Years 1996-2023. With this information, the Z-score was computed which indicated how much a specific value deviated from the mean (Mcleod, 2023). A Z-score describes the position of a raw score in terms of its distance from the mean when measured in standard deviation units. The z-score is positive if the value lies above the mean and negative if it lies below the mean (Mcleod, 2023).

It is calculated with the following equation:

$$Z = \frac{x-\mu}{\sigma} \hspace{4cm} Equation\ 1$$

Where:
- z = Z-score
- x = the value being evaluated
- μ = the mean
- σ = the standard deviation

From figure 2, the average precipitation for August was observed with a total of 81 mm. The monthly averages for April, May, and June are 37 mm, 49 mm, and 70 mm, respectively. In August 2023, the recorded precipitation was 158.7 mm, which is significantly higher than the typical average of 81 mm. In contrast, July had a precipitation of 88.4 mm, which is closer to

8

the average of 71 mm. April, May, and June experienced much lower precipitation rates of 13.4 mm, 12.6 mm, and 18.5 mm, respectively. The precipitation data for the Rönne å catchment area was obtained from the Hörby A weather station, which is located at a latitude of 55.8624, longitude of 13.6673, and an altitude of 112.8 m above sea level (SMHI, 2024).
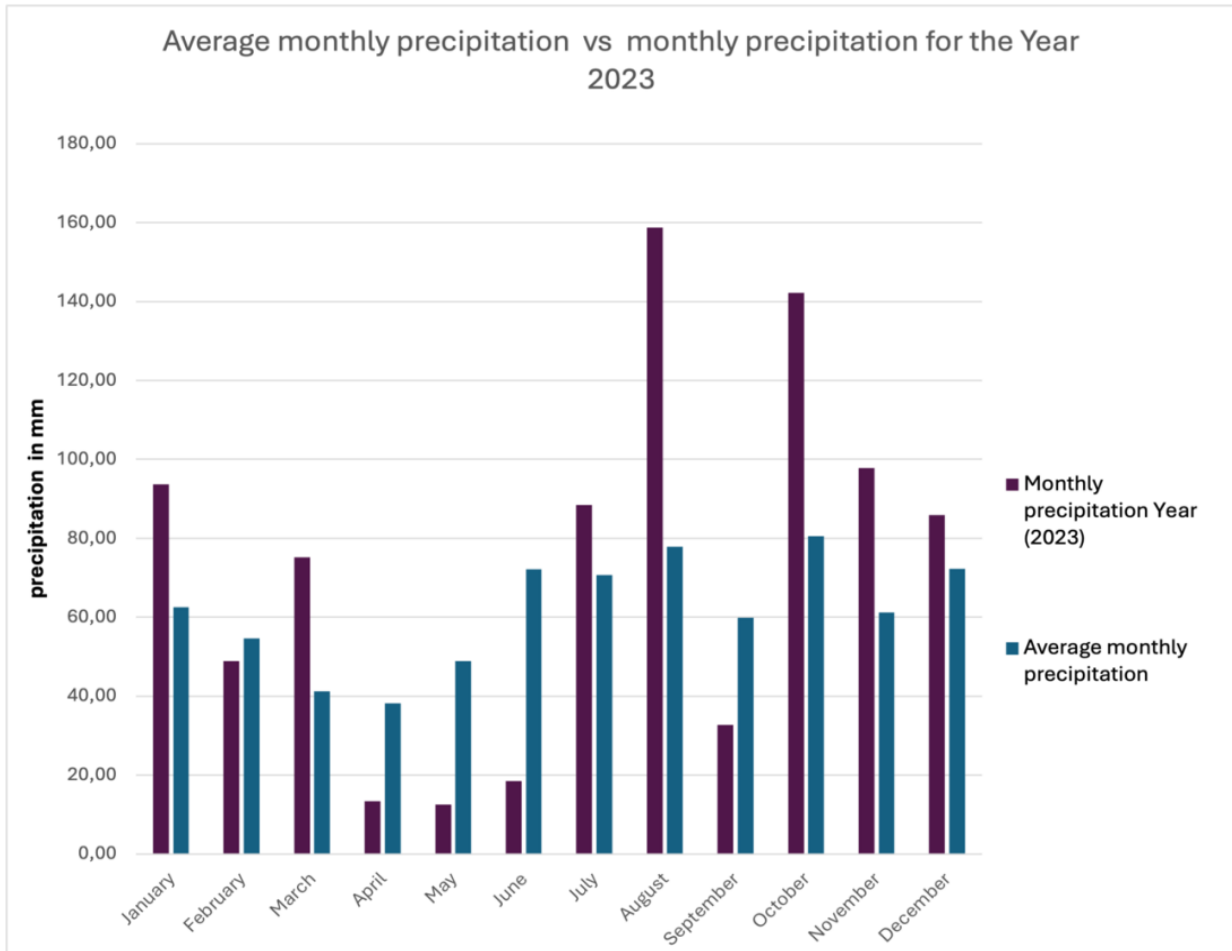

Figure 2: The average monthly precipitation (1996-2023) is depicted in blue and the monthly precipitation for the Year 2023 is shown in dark purple. The data was derived from of Hörby A Station (SMHI, 2024).

2.2.2 Multi-criteria analysis

MCA in Geographic Information Systems is a decision-making tool that integrates various layers of spatial data to evaluate multiple criteria simultaneously (Malczewski, 2006). It is widely used in environmental management and urban planning, where decisions must take into account various geographical and socio-economic factors. It enables the integration and analysis of various spatial data layers, which can facilitate and support complex decisionmaking processes (Rincón et al., 2018). Within MCA, methods like AHP, Weighted Linear Combination (WLC), and Fuzzy Sets play crucial roles. The AHP developed by Thomas L. Saaty in the 1970s, is a decision-making tool used in situations that involves multiple criteria and is used to prioritize and quantify criteria within a hierarchical structure (Saaty, 2008). It involves pairwise comparisons of criteria to establish their relative importance, which results in the calculation of weights that reflect the priorities of the decision-makers (Saaty, 1980). This approach is useful in scenarios like flood risk management, where multiple variables must be considered to make informed and balanced decisions. WLC is a widely used method in an MCA, where each criterion is assigned a weight that indicates its relative importance and evaluates each option based on these criteria. Each criterion of the WLC is then overlayed together with their respective weight in order to produce a result. This method facilitates the comparison and ranking of different options based on multiple criteria (Malczewski, 1999). Fuzzy sets are used to normalize the values of the different criteria used in an MCA. They extend classical sets by incorporating partial truth, where truths can range between completely true and completely false (Zadeh, 1965). A fuzzy membership function quantitatively represents the degree to which a factor belongs to a set on a continuum between 0 and 1. This approach more accurately reflects the natural world than assigning precise values and hard limits to factors (Zadeh, 1965). Following the methodology of the papers from Ali et al. (2023), Noori & Bonakdari (2023) and Hagos et al. (2022), the following factors for the MCA were considered: Elevation, Slope, Precipitation, Drainage Density, Proximity to river, Soil Type/Texture and Land use/cover. In this paper, weights from previous studies were used for flood risk assessment. Those articles were chosen because they present similar factors despite being from different geographic and climatic regions. This may indicate that their weights and factors can be applicable across various climatic conditions. Furthermore, one analysis was assigned equal weights. Thus, based on the values from the previously mentioned articles, the following weights were used:

Table 2: The various weights utilized for the flood risk assessment. One set of weights was derived from a study conducted in Tunisia by Ali et al. (2023), while another set was based on research from Ontario by Noori & Bonakdari (2023). Another set of weights was taken from a paper from Ethiopia by (Hagos et al. 2022). The final set of weights was evenly distributed across all factors.

Factor	Ali et al. (2023)	Noori & Bonakdari (2023)	Hagos et al. (2022)	Equal weights
Slope	0.14	0.16	0.38	0.14
Elevation	0.39	0.04	0.23	0.14
Drainage density	0.25	0.10	0.14	0.14
Proximity to river	0.09	0.10	0.10	0.14
Rainfall	0.02	0.29	0.06	0.14
Soil texture	0.06	0.16	0.04	0.14
Land use	0.09	0.12	0.02	0.14
Sum	1	1	1	1

After the weights for each factor has been assigned, every factor was normalized with the help of fuzzy sets. In this paper, a linear membership function has been used for all continuous factors including slope, elevation, precipitation, drainage density, and proximity to rivers. A positive linear membership function has a positive slope, meaning as the input value increases, the membership value also increases. Conversely, a negative linear membership function has a negative slope, where the membership value decreases as the input value increases (Zadeh, 1965). Categorized data such as soil texture and land cover were assigned values between 0 and 1 based on their effect on flooding.

All continuous data was normalized according to the following equation:

Equation 2

$$\mu_A(x) = \begin{cases} 0 & \text{if } x \leq a \\ \frac{x-a}{b-a} & \text{if } a < x \leq b \\ 1 & \text{if } x > b \end{cases} \qquad \mu_A(x) = \begin{cases} 1 & \text{if } x \leq a \\ \frac{b-x}{b-a} & \text{if } a < x \leq b \\ 0 & \text{if } x > b \end{cases}$$

a   *b*

Where:

- µA(x) = Membership function of fuzzy set A
- x = Input variable, representing the value for which the membership degree is being calculated
- a = Lower bound of the interval where the membership function changes
- b = Upper bound of the interval where the membership function changes

Equation 2 (a) was used to normalize factors which followed a positive fuzzy membership, which is shown as the blue line in figure 3. Controversy, factors that followed a negative fuzzy linear membership were computed with equation 2 (b) and is visually represented as the red line in figure 3. In this paper, normalized values close to 0 can be understood as very low flood risk and values close to 1 as very high flood risk.
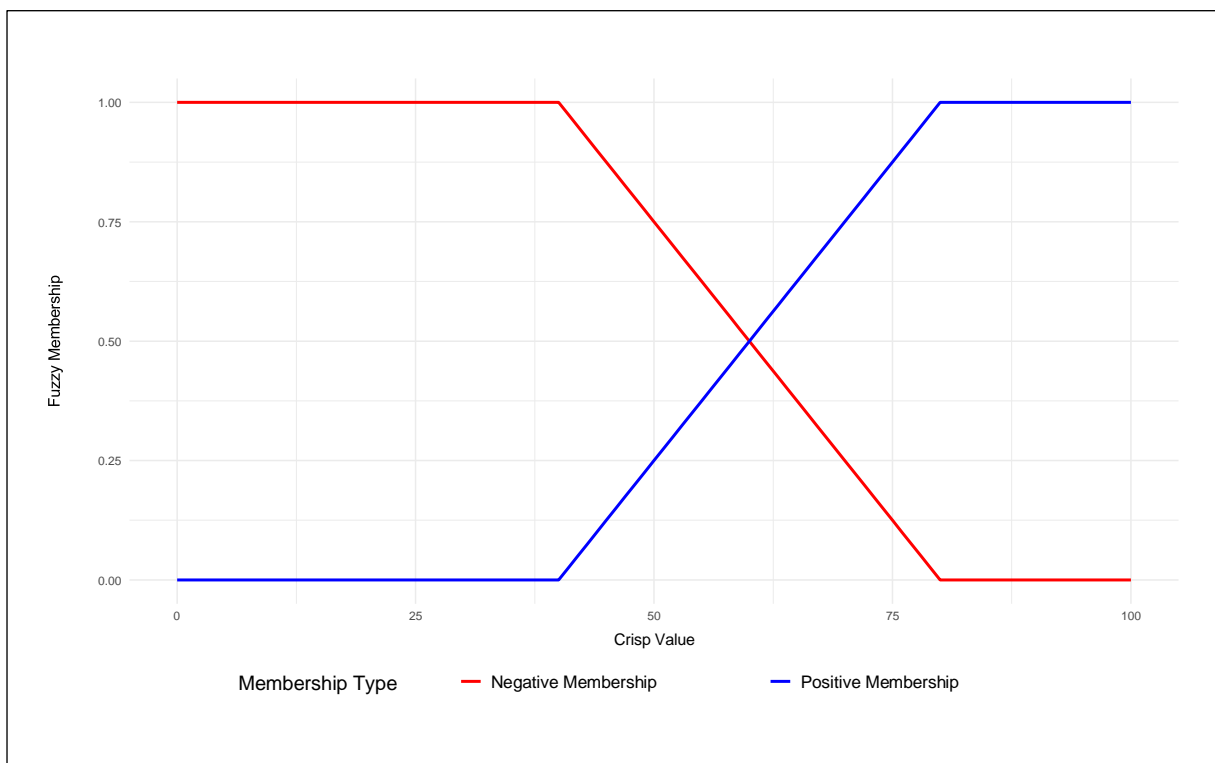
Figure 3: The blue line is representing a positive fuzzy linear membership whereas the red line is showing a negative linear fuzzy membership.

After the different weights for each of the factors were chosen and normalized according to fuzzy linear equations, all factors were combined using WLC, which is described in the following equation:

Flood hazard = $\sum W_i X_i$ *Equation 3*

Where:
  * W_i = weight of factor *i*
  * X_i = criterion score of factors *i*

With equation 3, all normalized factors were assigned their respective weight and summed to produce a final flood risk map. The outcome of the MCA produced four different maps, one based on the weights from Noori & Bonakdari (2023), one from Ali et al. (2023), Hagos et al. (2022) and the last one where all factors were set to equal weights. All layers were snapped to the Rönne å catchment from SMHI (2016) with a resolution of 10m. The resulting flood risk maps were compared with the flood map based on MIKE 11 from Sweco (2014).

2.2.3 Factors used in the MCA

2.2.3.1 Slope
Slope refers to the inclination or gradient of a surface or land area and is typically expressed as a percentage or as degrees (Hagos et al., 2022). It is an important indicator describing the vulnerability of the region to flooding as it indicates the rate and duration of water flow (Ali et al., 2023; Kaya & Cengiz, 2023). In areas with low slopes, water moves more slowly and thus accumulates on flatter surfaces making it more prone to flooding compared to steep slopes (Ali et al., 2023). Furthermore, it affects the quantity of surface runoff generated by precipitation which is crucial when assessing flood risk in an area (Hagos et al., 2022). The slope values were normalized according to the fuzz linear function in equation 2 where all slope values above 12° were assigned no risk. The slope map has been created in ArcGis pro 2.7.0 with the spatial analysis tool "slope", and a DEM layer of a 2m resolution which was provided by Läntmateriet (2019).

2.2.3.2 Elevation
Digital Elevation Models (DEM) play an important role in assessing vulnerable area to flooding. Generally, higher elevation areas are less prone to flooding compared to lower lying areas, where water tends to accumulate (Hagos et al., 2022). The resolution of the DEM also plays a significant role when it comes to the accuracy of the flood risk map (Van De Sande et al., 2012). The DEM for the Rönne å catchment area was provided by Läntmateriet (2019), with a resolution of 2m. In a GIS environment, the DEM values were assigned a value between 0 and 1 based on their influence on flooding. In this paper, the highest elevation of 227m was assigned a fuzzy value 0 which increases with decreasing elevation where no elevation was assigned the fuzzy value 1.

2.2.3.3 Drainage density

Drainage density is an important factor in flood risk mapping as it significantly influences how quickly surface runoff reaches streams and rivers (Liu et al., 2019). It refers to the total length of all the streams and rivers in an area divided by the total area of the drainage basin and can be understood as an inverse function of soil permeability (Hagos et al., 2022). High drainage density values indicate low infiltration rates and higher surface flow velocity and surface runoff, hence high flood risk (Ali et al., 2023; Shuaibu et al., 2022). As shown in the equation below, drainage density is the total length of the stream segments divided by the unit area (Hagos et al., 2022):

$$Dd = \frac{\sum_{i=1}^{n} L_i}{A} \hspace{4cm} Equation\ 4$$

Where:

- $\sum_{i=1}^{n} L_i$ is the total length of drainage in kilometers,
- *A* is the total area of the study site in square kilometers (km^2),
- *n* is the number of drainage networks in the watershed.

In a GIS environment, drainage networks have been extracted from DEMs with a resolution of 2 m using a spatial analysis tool in ArcGIS Pro 2.7.0. The generated drainage networks have been compared with the available river network data from SMHI (2016) and it was decided to use the latter due to their similarity. From that, Line Density was used to calculate drainage density area from stream polyline features (Ali et al., 2023). The population field was set to NONE, and the search radius was set to default. The search radius determines the "neighborhood" around each cell for which the density is calculated. The default search radius is typically set to the shortest dimension (width or height) of the output raster's extent divided by 30 (ESRI, n.d.). This default ensures that the search radius is proportional to the size of the analysis area, providing a balance between local and broader spatial influences.

2.2.3.4 Proximity to river

Distance to water bodies is an important factor in the analysis of flooding risk. This is because riverbanks and areas close to waterbodies are more vulnerable to flood impacts than areas further away from rivers (Ali et al., 2023). Areas that are within 500m from rivers represented a very high hazard of floods as indicated by (Osman & Das, 2023) and the flood risk diminished linearly with increasing distance to streams where areas further than 3000m from streams were set to very low risk. In a GIS environment, a stream network was derived from a 2m resolution DEM. With the aid of the hydrological tools in ArcGIS Pro 2.7.0, flow direction and flow accumulation were calculated. From the flow accumulation raster, a stream network was delineated with the help of the "con" tool, where all cells with more than 100.000 cells flowing into them are assigned the value 1, and all other cells are assigned 'NoData'. This condition has been assigned due to the high resolution of the DEM. Had smaller values like 1000 or 10,000 been selected, the river network would appear overly clustered, obscuring any distinct network patterns. Furthermore, when overlaying the generated network layer with the downloaded layer from SHMI (2016), they looked very similar which was the defining factor to use this condition. From this, the Euclidean distance from each point in the Rönne å catchment area to water bodies was calculated (Ali et al., 2023). Since distance to rivers and its relation to flood risk does not have hard limits in the natural world, fuzzy linear was used to create a value between 0 and 1, where areas close to the river were assigned a high value which is decreasing with distance.

2.2.3.5 Precipitation

Precipitation plays a crucial role in flood risk mapping because it directly influences the volume of water that an area must manage during precipitation events (Bracken et al., 2007). In this paper, the monthly precipitation of August 2023 was utilized. To obtain spatial precipitation data, 200 interpolated precipitation points were downloaded from SMHI (2024) website and imported as into ArcGIS as a table. The table was exported as a point layer over the catchment area. The data was then interpolated with a bilinear interpolation method with a cell size of 10m and for the August precipitation values. The output provided a spatial precipitation raster layer for the month of August 2023 in mm. The precipitation data was transformed into fuzzy linear values that range between 0 and 1, where the values were sorted according to the average precipitation of the month of August in the Rönne catchment.

As precipitation values which are 2 std. above the mean can be understood as extreme precipitation, the precipitation values were normalized according to the following equation:

Extreme precipitation = average precipitation + 2 × std.   *Equation 5*

Substituting the given values:

Extreme precipitation $= 81mm + 2 \times 46$ = 173 mm. Thus, for all precipitation values >= 173mm, Fuzzy value = 1

2.2.3.6 Soil texture and Infiltration rate

Soil texture is a key factor in flood risk management as it directly influences the infiltration rate and water retention capacity of the soil (Jarrett & Emeritus, 2022). It refers to the relative proportion of sand, silt, and clay size particles in a sample of soil (Ritter, 2022). The relationship between soil texture and infiltration rate is significant because the size and distribution of soil particles affect how quickly and effectively water can move into and through the soil (Jarrett & Emeritus, 2022). Sandy soils, with their larger particle sizes and greater pore spaces, allow for quicker water infiltration and faster drainage. This reduces the likelihood and severity of flooding by minimizing surface runoff. In contrast, clay soils have smaller particles and tighter pore spaces, leading to higher water retention but lower infiltration rates. This can cause increased surface runoff and a higher risk of flooding during heavy rainfall events, as water is less efficient at penetrating the soil quickly and accumulates on the surface instead (Jarrett & Emeritus, 2022). Thus, areas with high infiltration capacities tend to have reduced peak flows and lower flood magnitudes due to their ability to absorb more water (Hernández-Atencia et al., 2023). Conversely, when areas predominantly covered impervious soils or bedrock the infiltration capacity of the soil decreases, leading to higher surface runoff, which can increase the peak flow rates and, subsequently, the likelihood and severity of flooding (HernándezAtencia et al., 2023). Based on this information, combined with the soil-texture triangle provided by Phillips (2023), the relationship between soil texture and infiltration rate was established. The soil type layer provided by SGU (2023) has been translated according to Table 9 in the appendix. The various soil types have then been grouped based on their soil texture, drainage capacities, and their impact on flooding. In this paper, the soil's impact on flooding was categorized according to the table below, which categorizes soil types by their effect on flooding, ranging from very low to very high. The specific soil types in each category are detailed in the appendix, Table 9:

Table 3: The different soil categories, their infiltration rate and respective contribution to flooding.

Soil type	Infiltration rate	Soil / Rock Categories	Contribution to flooding
Sand	Very high	Sandy Soils	Very Low
Loamy sand	Very high – High	/	/
Silt	High	Silty Soils	Low
Sandy loam	High - Moderate	/	/
Silt loam	Moderate - High	/	/
Loam	Moderate	/	/
Sandy clay loam	Moderate - Low	/	/
Silty clay loam	Low - moderate	/	/
Sandy clay	Low	/	/
Silty clay	Low - Very Low	/	/
Clay loam	Very Low -Low	/	/
Clay	Very low	Clay Soils	Very high
Peat soils	Moderate	Peat Soils	Moderate
Gravel	High - Moderate	Gravel and Coarse Material	Low - Moderate
Rock types	Low – Very Low	Rock types	High
Other	No Value	Water and Artificial Fills	No value

2.2.3.7 Land cover

Land cover plays a significant role in influencing flood risk due to its impact on surface water runoff and infiltration. Urban areas, characterized by high levels of impervious surfaces like roads and buildings, typically experience lower infiltration rates, which increases runoff and enhances the risk of flooding. Conversely, areas with natural vegetation or permeable surfaces can help mitigate flood risks by enhancing water absorption and reducing runoff (Gabriels et al., 2022). Wetlands can retain flood waters temporarily during periods of high runoff. As the flood waters diminish, the retained water is gradually discharged from the wetland soils. By capturing and decelerating the flow of flood waters back into stream channels, wetlands can help to diminish the impact of downstream flooding (DEC 2024). The land cover data of the

Rönne å catchment area has been provided by NMD (2018) and has been merged into the following groups (table x). This was done by putting each class from the layer into its respective group which has been decided based on its definition from NMD (NMD, 2020). The respective classes found in each group can be found in the appendix (Table 10):

Table 4: The different land cover categories and their respective effect on flooding.

Land use Categories	Effect on flooding
Wetland	Very low
Forest	Low
Open land	Moderate
Agricultural land	High
Build up	Very high
Inland water	No value

2.2.4 Flood map based on MIKE 11

In this paper, the created flood risk maps from the MCA were compared with a flood map from Sweco. The flood risk map that was produced by Sweco (2014) used a model that contains information about flows, elevation data and structures in the watercourse such as bridges and dams and other physical structures that affect the water movements (DHI, 2023). Sweco used the hydrodynamic model MIKE11, which is based on Saint-Venant equations to simulate water flow and flood events over time and includes detailed factors such as as slope, bottom friction as well as the topography of the landscape (Sweco 2014). Finally, the model is calibrated against previous measurements of water level and water flow. From all this information, their map has been created. Thus, this model used a significantly different approach when it comes to modeling flood risk in comparison to the MCA and computed different outputs. In this paper, the hydrodynamic model was based on a 200-Year flow event (Sweco 2014). While the MCA produced a flood risk map showing areas with different relative risk levels, MIKE 11 produced dynamic, time-based simulations of flood extends and depths, offering more precise flood predictions.

3 Results

3.1 Extreme Precipitation

Table 5: Monthly average precipitation of Hörby A Station from 1996-2023 for the month of August, its standard deviation and the respective Z-scores for the selected Year 2023 (SMHI, 2024).

Variable	Value
Average	81
Std	46
Z-score_August (2023)	1.68

Z-score for the month of August 2023 was calculated (equation 1). This was done with the help of the standard deviation (std) for the month of August, which is 46. From that, the Z-score was calculated for the month of August, which turned out to be 1.68 (table 6). This means that the value for the Year 2023 is 1.68 standard deviations above the mean value of the month of August (Mcleod, 2023). Since 2 std above the mean can statistically be defined as extreme precipitation, the month of August (2023) with its 158mm of rainfall is trending towards significance. Thus, for this paper, it was categorized as an extreme precipitation event.

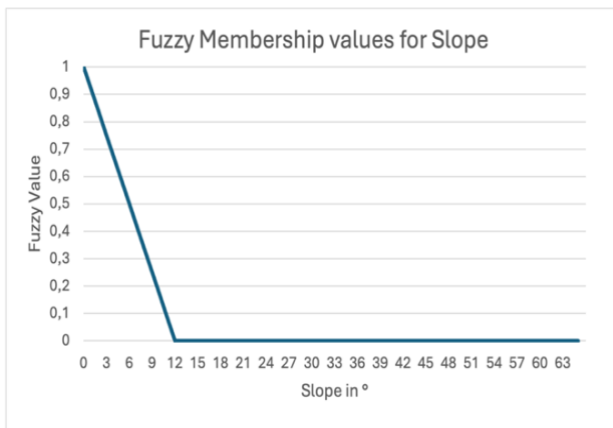## 3.2 Fuzzy membership functions

The following figures are showing the different linear membership functions for each continuous factor. For proximity to river in figure (4d), all values below 500m were assigned value 1 and decreased until 3000m, where it was assigned the value 0; 1 being high and 0 being low flood risk. For the elevation, there is a continuous decrease in the fuzzy value with an increase in elevation. The highest elevation of 227m was assigned the value 0 and 0m the value 1. As for Drainage density in figure (4c), there was linear increase in the fuzzy value from 0 – 0.4. At a drainage density of 0.3 km/km^2, the assigned fuzzy value was 1, meaning a high effect on flooding. Like Drainage density, extreme precipitation also follows a positive linear fuzzy

membership function figure (4e), where a precipitation of 173mm was assigned a fuzzy value of 1. Slope in figure (4a) followed a negative membership function. A slope of 0 was assigned a fuzzy value of 1 which was decreasing with an increase of slope. At a slope of 12°, the effect on flooding is very low and thus was assigned the fuzzy value of 0 onwards. For categorized data such as land cover and Soil type, each class was assigned a number between 0 and 1 based on their effect on flooding:

Table 6: Assigned membership values for each land cover and soil type class based on their effect on flooding.

| Land Cover	Soil type	Effect on flooding	Assigned membership values
Wetland	Sandy Soils	Very Low	0
Forest	Silty Soils	Low	0.25
/	Gravel, Coarse Material	Low - Moderate	0.37
Open Land	Peat Soils	Moderate	0.5
Agricultural Land	Rock	High	0.75
Build up	Clay Soils	Very High	1
Lake	Water / Artificial Fill	No effect	No Value

All continuous data was normalized according to the following linear functions:
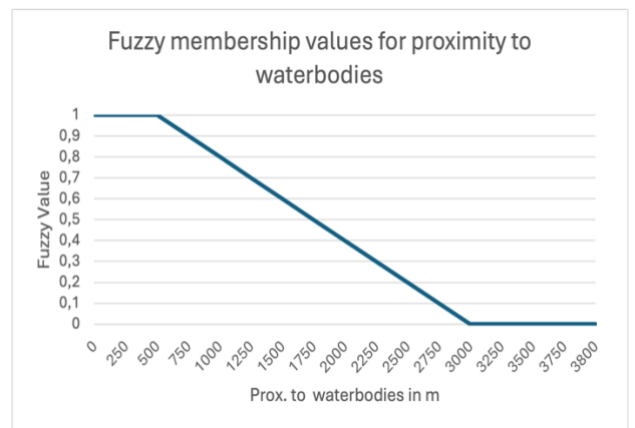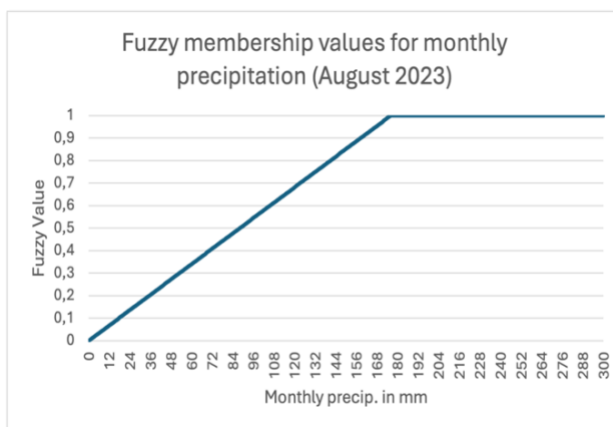
a
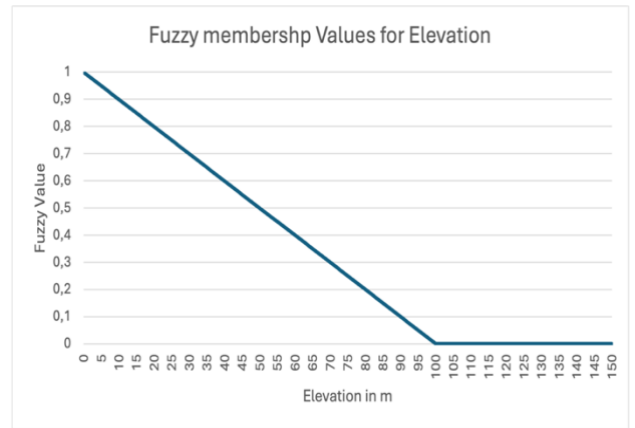
b
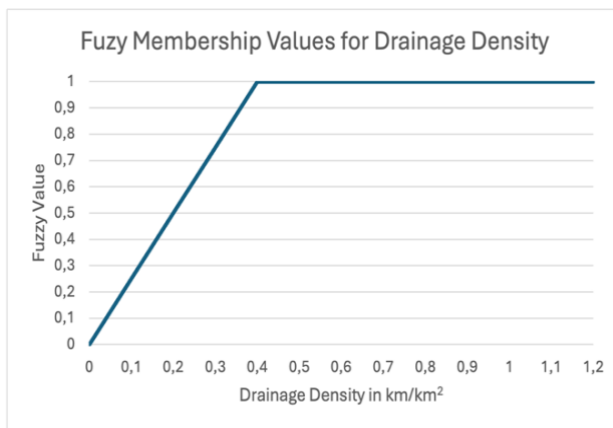
c

d

e

Figure 4: Fuzzy membership functions for all continuous factors. The fuzzy slope shows a negative membership (4a), so does proximity to river (4d) and elevation (4b). Drainage density and monthly precipitation show a positive membership function (4c, 4e).

3.3 Multi-criteria factors

The natural ranges for the slope, elevation, drainage density and proximity to river factors are displayed in figure 5. The Rönne å catchment presented a relatively low elevation that ranged from 0m to 227m. The east of the catchment generally showed higher elevation values than the west where the Rönne å river flows. The slope varied from 0° to 65°. It is generally scattered across the catchment with some areas of high slope values in the north and mid-east of the catchment. It also seemed to follow a pattern of low slope values along river networks. For the proximity to river factor, the longest distance from a river was at 3718 m. This factor very closely followed the natural river network where areas close to rivers had low values (figure 5). The drainage density varied between 0 and 1.2 km/km^2. If not as clear, drainage density showed areas of high drainage density along the main river network patterns and was evenly distributed across the catchment.
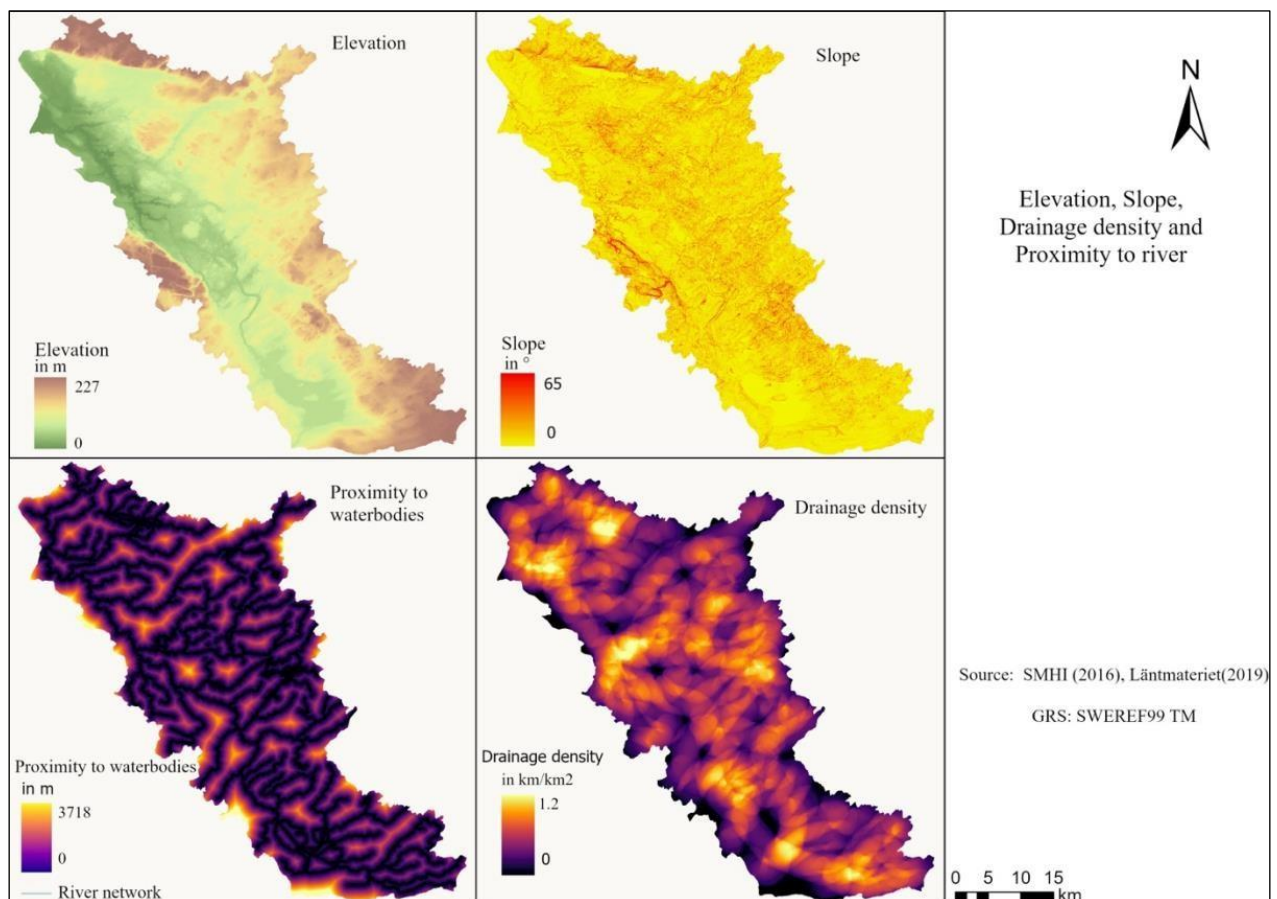

Figure 5: Values for the different continuous factors including elevation, slope, proximity to waterbodies and drainage density. Proximity to waterbodies and elevation is expressed in m, slope in degrees and drainage density in km/km².

The normalized values for elevation, slope, proximity to waterbodies and drainage density are represented in figure 6. All those factors are represented according to their assigned fuzzy values, where areas close to 0 represented a very low flood risk whereas areas closer to 1 represented high risk areas for flooding. figure 6 showcased that areas close to the rivers have higher flood risk, following the general river network pattern. Slope and elevation also presented high risk areas around the Rönne å river since it is in a valley that had relative low slope and elevation values. Generally, the normalized values for elevation show a higher risk in the west of the catchment compared to the rest. This correlated with the actual elevation of the area in figure 5, as they were areas with the highest elevation in relation to the rest of the catchment. Slope shows low fuzzy values in regions of high slope degree and seemed equally distributed across the catchment with some areas of little to no slope along the Rönne å river and main waterbodies.
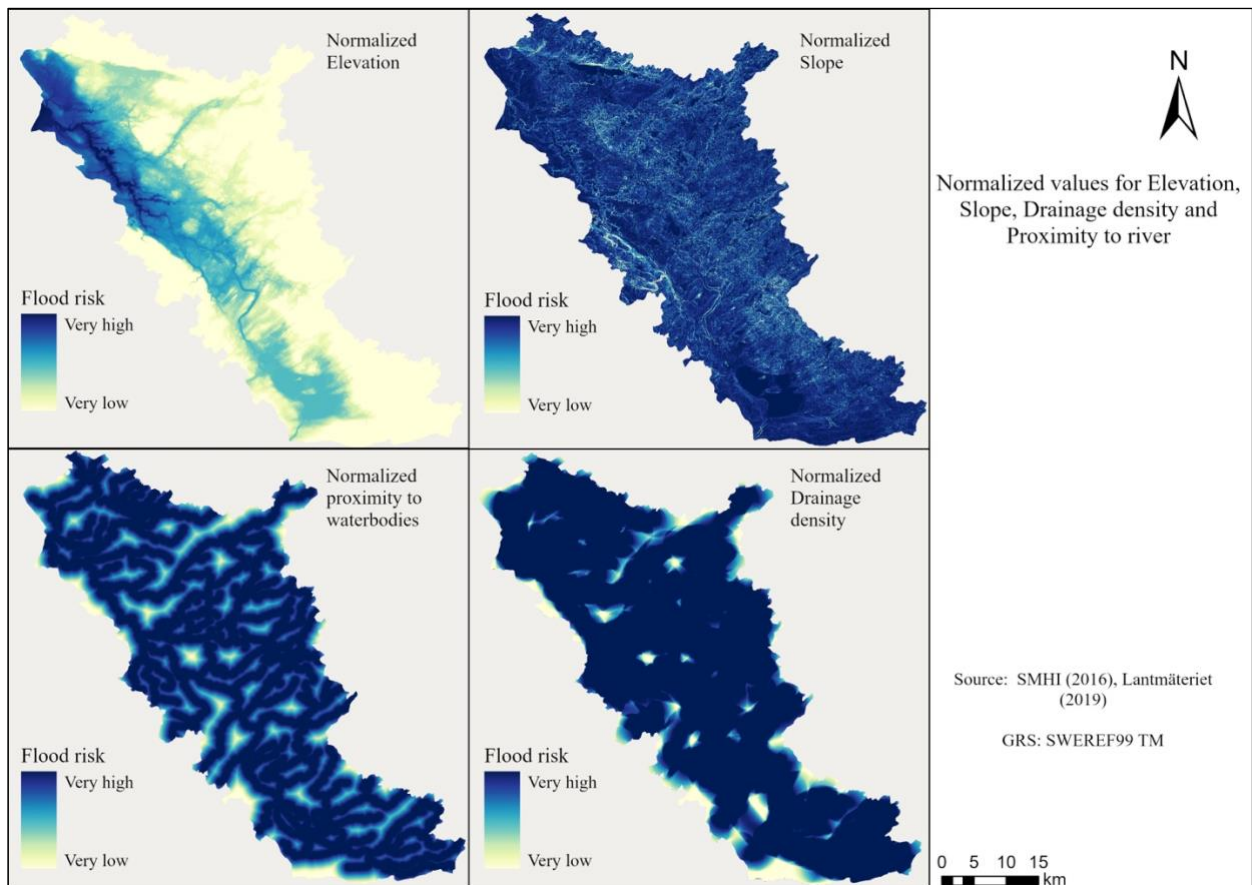

Figure 6: Normalized values for the following continuous factors: elevation, slope, proximity to river and drainage density. The values ranged between 0 and 1, where 1 equals to Very high risk (areas in dark blue) and 0 equals to very Low risk (areas in light beige).

The spatial distribution of the precipitation? in the Rönne å catchment for the month of August (2023) and its normalized values to assess its effect on flooding are displayed in figure 7. Since the catchment presented a relatively small area of 1897 km^2, there was limited spatial variation in precipitation expected. The highest amount of precipitation was found close to the Kattegat Sea with an amount of 334mm and the lowest amount was found in the southeast of the catchment area with 162mm of monthly precipitation. As all precipitation values above 173mm were assigned the fuzzy value 1, there was limited spatial variation of the normalized precipitation values across the catchment to be observed. This showed that for the month of August 2023, almost the entire catchment area experienced high risk to flooding from a precipitation perspective.
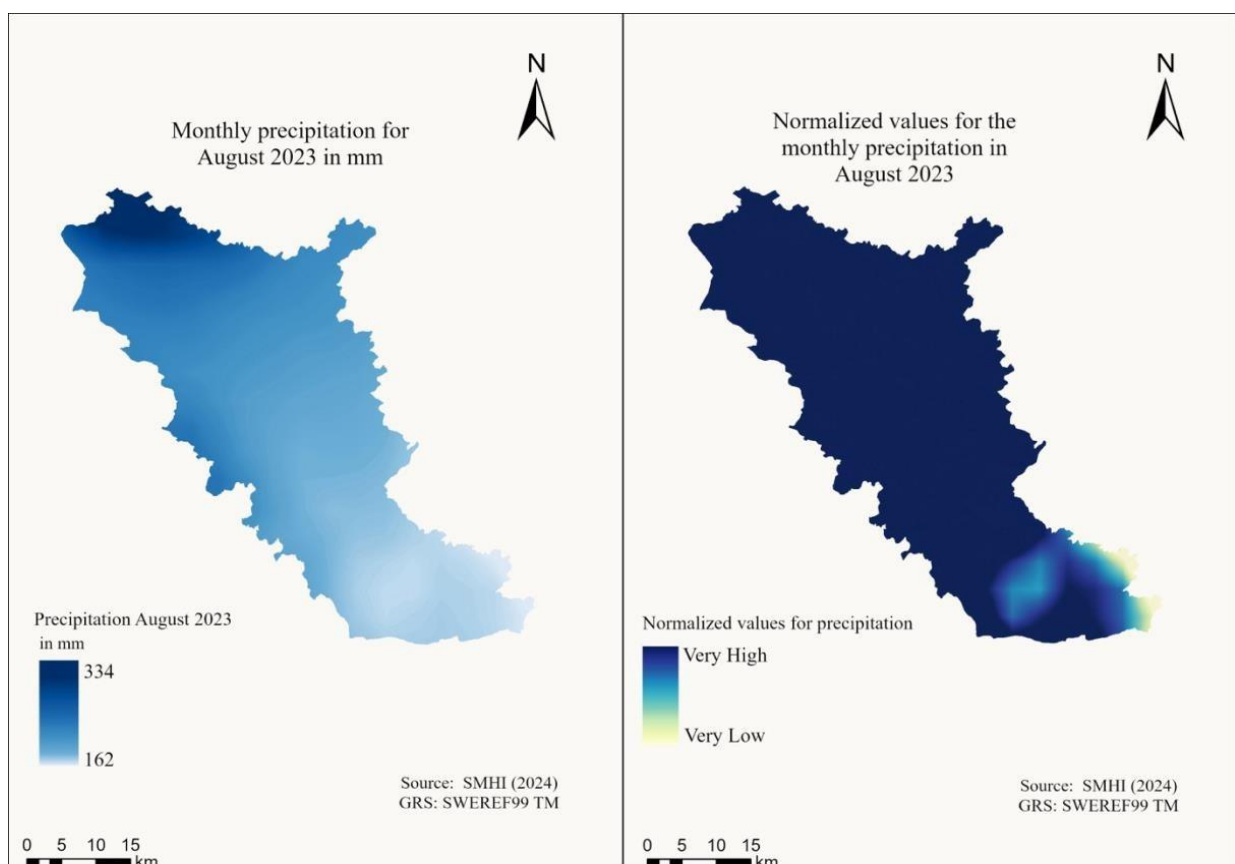
Figure 7: The monthly precipitation for the month of August 2023 and its respective effect on flooding based on normalized values ranging from Very Low to very High. Monthly precipitation was expressed in mm.

 The spatial distribution for soil types and land cover, together with their effect on flooding is represented in figure 8. From visual inspection, it was possible to recognize that clay soils were found in agricultural areas, which was mostly found in the west of the catchment. Forest covers the biggest area with a total of 37% of the total catchment, followed by agricultural and open land with 23% and 22% respectively figure 9 a. From figure 9b, it was found that sandy soils

were the most prominent and covered 68% of the total catchment area, meaning that most of the catchment contained soils with high infiltration rates. This was also observable in figure 8 where all dark blue areas represent sandy soils and were assigned the value 0 meaning very low flood risk.
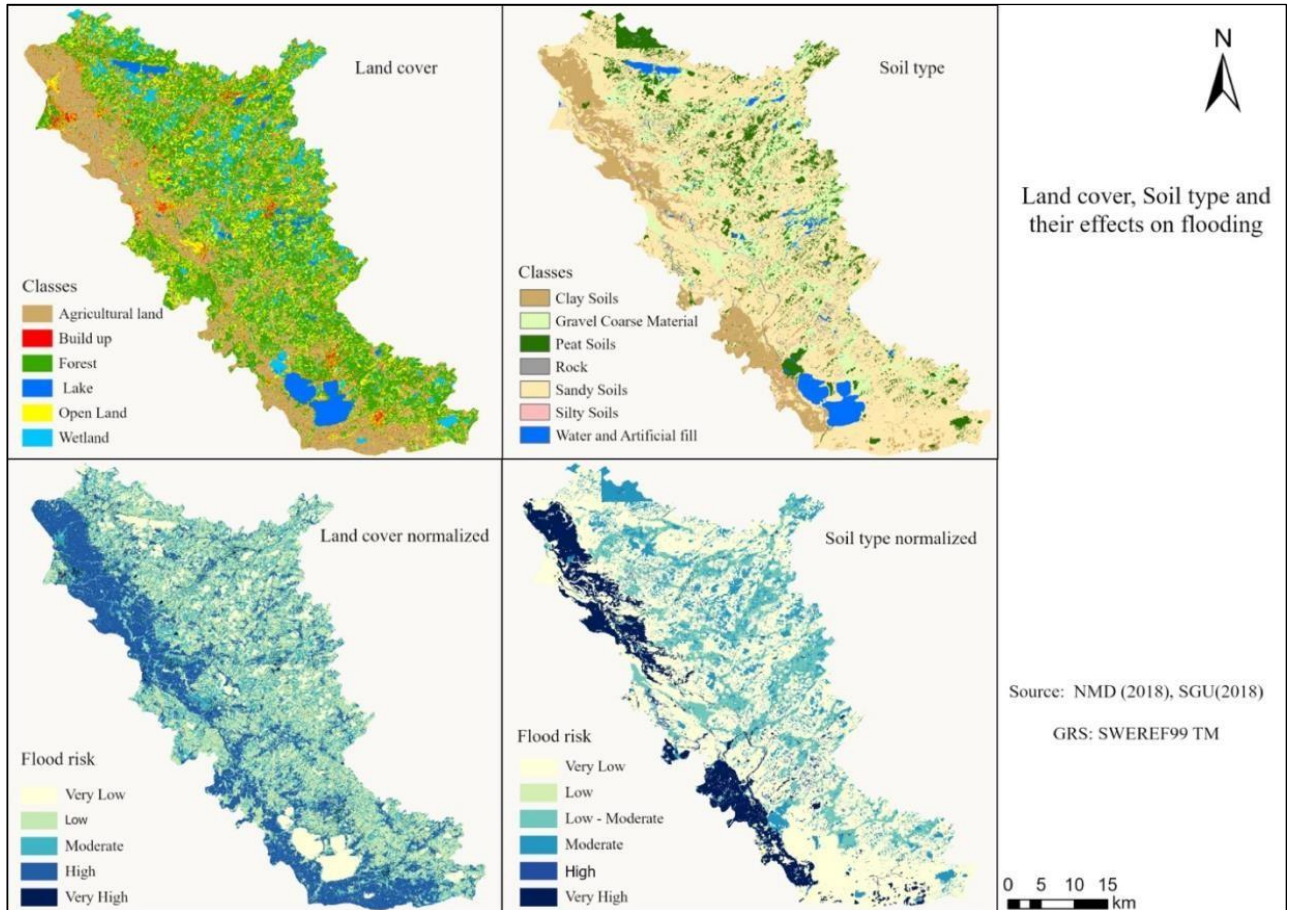
Figure 8: Spatial distribution of the different soil type and land cover classes across the catchment area. It also presented their respective normalized values that translated into flood risk ranging from very low to very high.

The following pie charts show the distribution of land cover and soil types:
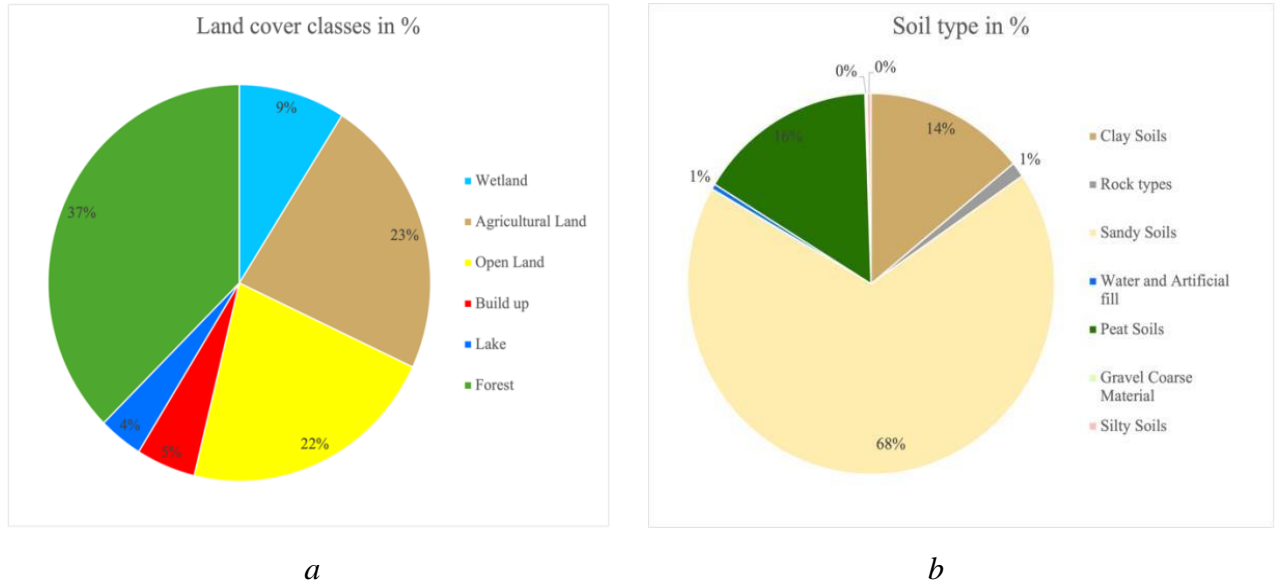
Figure 9: Distribution of land cover and soil type classes across the catchment in %, where (a) is showing the distribution if the land cover classes and (b) the distribution of soil type classes.

3.4 Flood Maps

Four different flood risk maps from the MCA were produced as illustrated in figure 10. Each map included relatively high-risk areas across the Rönne å catchment based on different weights from Ali et al. (2023), Noori & Bonakdari (2023) and Hagos et al (2022) and one flood map based on equally weighted factors. Values close to 1, presented areas that had a very high risk of flooding whereas values closer to 0 presented a low flood risk. When comparing the 4 maps, a clear pattern was recognized where areas in the west of the catchment illustrated higher risk areas compared to the rest of the river basin. Especially areas in the north-west demonstrated very high-risk areas for all produced maps. The map that was produced based on the weights

from Ali et al. (2023), showcased the biggest contrast between high and low risk areas, whereas the flood map based on the weights from Noori & Bonakdari (2023), turned out to produce a flood map with the most moderate-high flood risk areas across the catchment. The map produced by using the weights from Hagos et.al (2022) seemed to present the most high-risk areas close to the Rönne å river compared to the other maps. The map that was based on equal weights seems to provide a balance between the 3 other maps with selected weights.
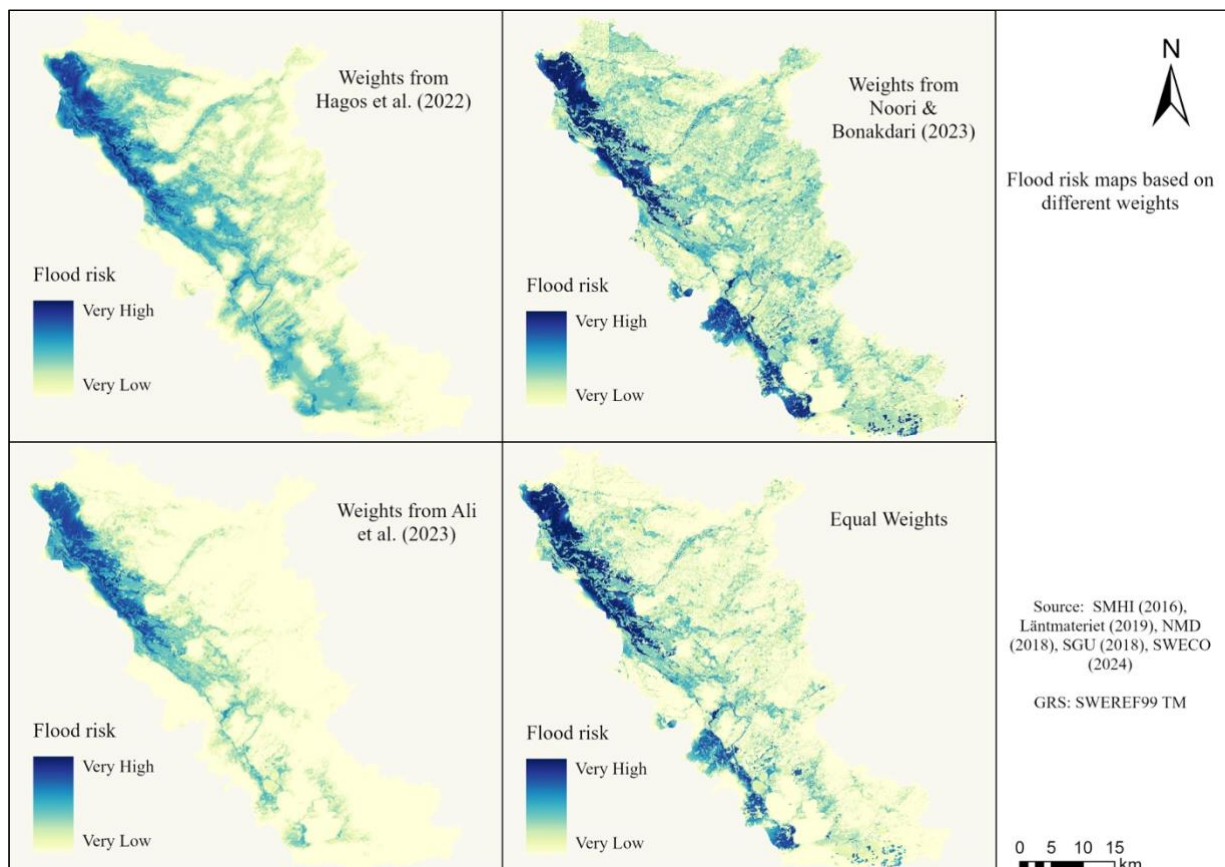
Figure 10: Relative high and low flood risk areas of the Rönne å catchment area based on different weights from Ali et al. (2023), Noori & Bonakdari (2023) and Hagos et al (2022) as well as a flood map based on equally weighted factors.

The maps in figure 11 showcase the same results than the one in figure 10. The difference between the 2 is that in figure 11, the flood risk maps were classified into very low, low, moderate, high, and very high flood risk areas. This provided a better overview on which areas are under very high risk and which are under no immediate flood risk. All 4 maps have been classified according to the natural breaks tool.
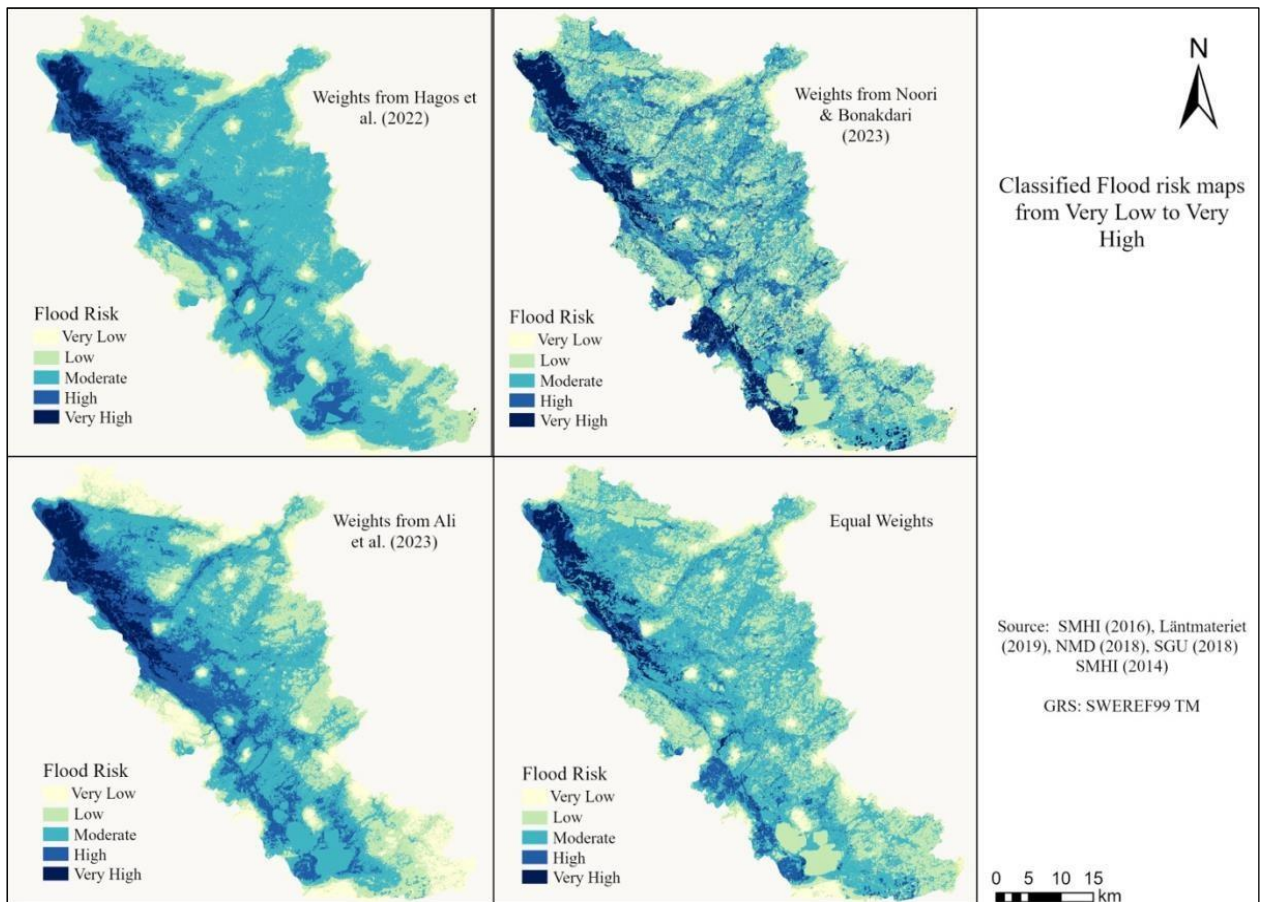
Figure 11: Classified high and low flood risk areas ranging from very low risk (light beige) to very high-risk areas (dark blue). The produced flood risk maps show the relative risk across the catchment and the classes have been produced using the natural breaks. The produced maps are based on weights from Ali et al. (2023), Noori & Bonakdari (2023) and Hagos et al (2022) as well as a flood map based on equally weighted factors.

The different percentages of each risk class based on the different weighting approaches were calculated and are illustrated in figure 12. From that, it was possible to conclude that the

distribution of the different relative risk classes based on the different weights follow a similar pattern, where the high-risk areas only vary between 5% figure 12(a) and 12(b), and 8% in figure 12(d). The flood map from Ali et al. (2023) presented the biggest area of very low risk class with 13% which is showcased in figure 12(c).

3.5 Comparison with the flood map produced by Sweco

Figure 13 is comparing the 4 produced flood risk maps from the MCA with a flood map from Sweco (2014) who based their map on the hydraulic model MIKE 11. When analysing the different maps, it was possible to recognise that the map created from the weights based on the article of Ethiopia (Hagos et.al 2022) aligns best with the MIKE 11 model. This observation was made by comparing the extent of the Model which can be seen as the red line in figure 13 and high-risk areas which are represented as dark blue in the produced flood risk maps. The map that was produced based on the weights from Ontario seems to have the least similarities with the MIKE 11 model. The result of the map based on equally distributed weights across the factors also seemed to provide a less accurate result when comparing it with MIKE11. The map based on the weights from Tunisia, provided the second-best results when comparing the very high-risk areas with the hydraulic model.

a

b

c

d
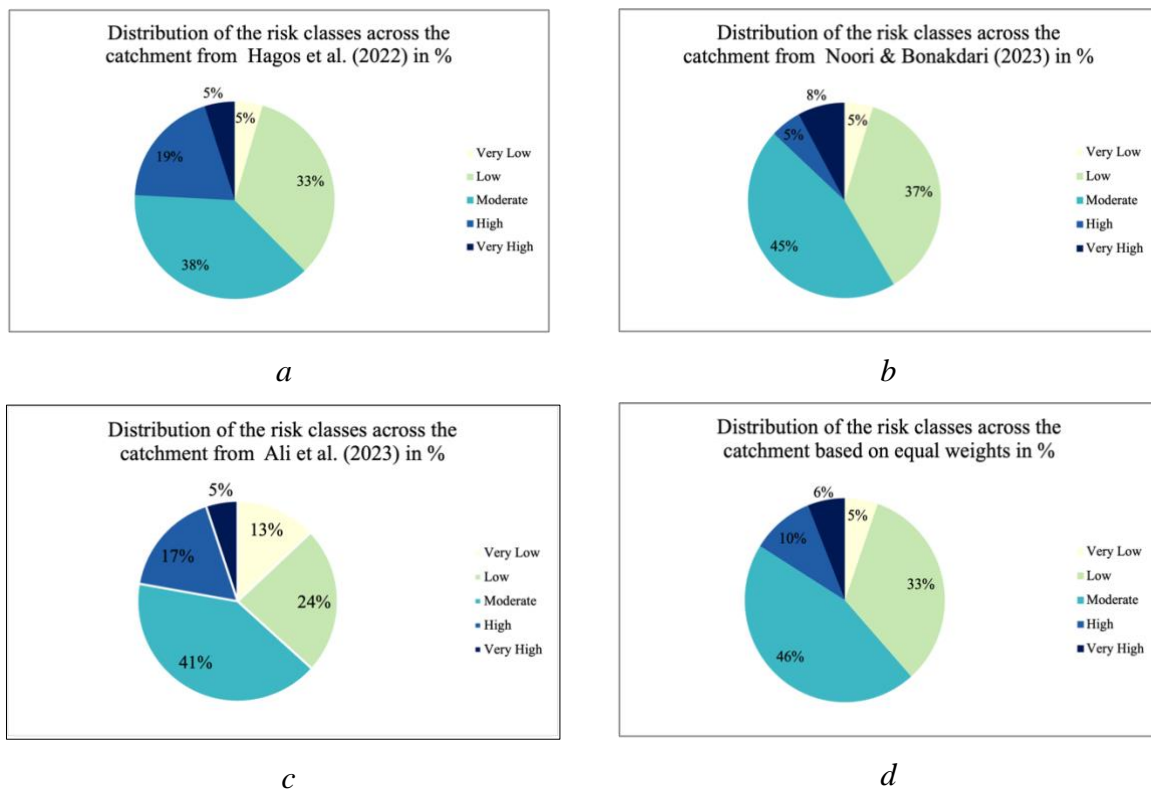
Figure 12: Spatial distribution of the different risk classed across the catchment area. There are 4 results, one based on weights from Hagos et al. (2022) (a), Noori & Bonakdari (2023) (b), Ali et al. (2023) (c) and one based on equal weights(d).
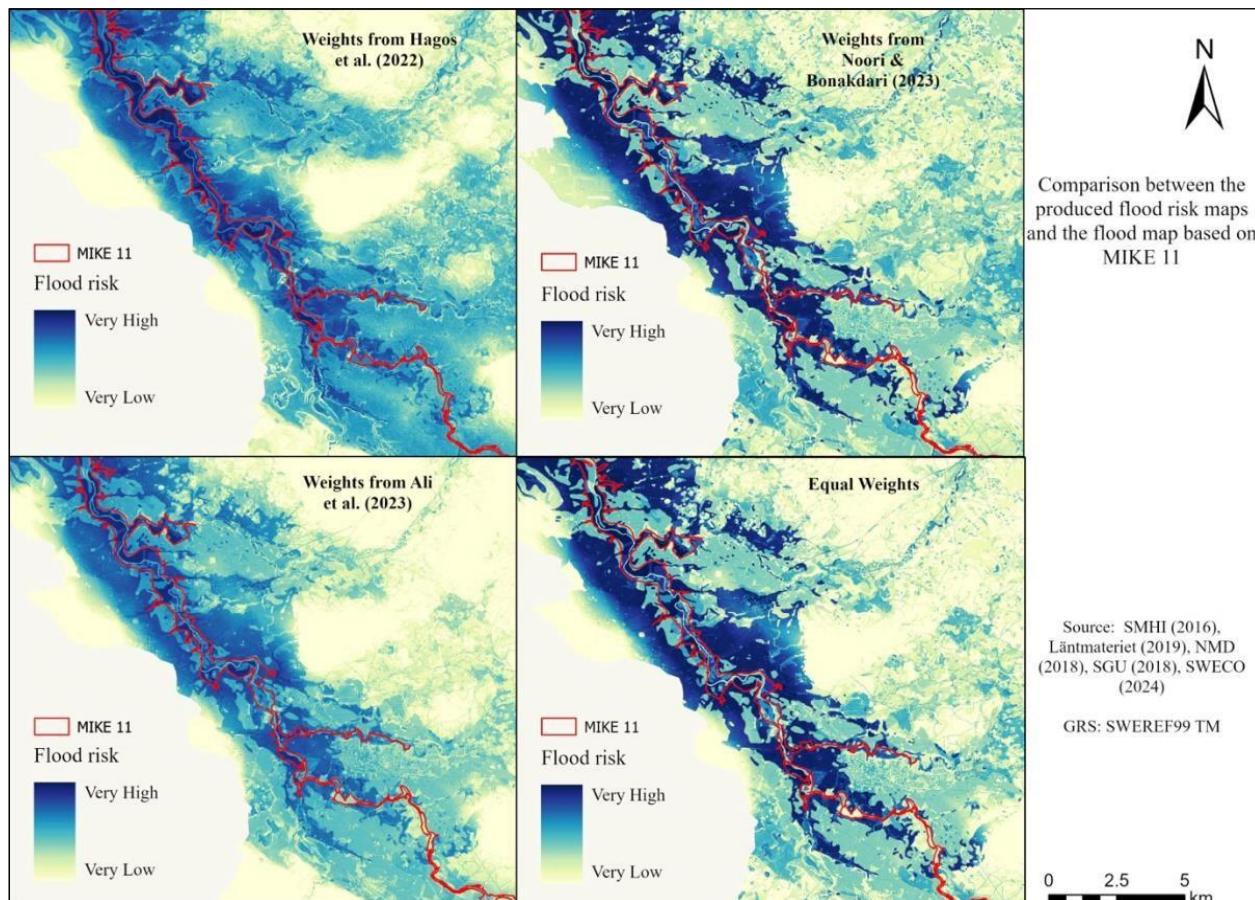
Figure 13: Comparison of the produced flood risk maps based on different weights with the Flood map from Sweco (2014) based on MIKE 11. The red outline represents the extent of the flood map from the MIKE 11 model.

The polygon layer resulting from the flood map produced by Sweco (2014), representing the red outline in figure 13, was overlayed with the classified flood risk map. This provided a ratio of how much of each flood risk class is contained in the polygon layer as presented in figure 14. The flood map created from the weights based on Hagos et.al (2022) ended up having the biggest ratio of high-risk areas in that polygon with 30% of very high-risk classes as shown in figure 14 (a). The flood map based on equal weights and the one resulting from Noori &

Bonakdari (2023 presented the smallest areas of high-risk classes, with a ratio of 17% and 18% respectively as illustrated in figure 14(d) and 14(b). The map produced based on Ali et al. (2023) presented a moderate amount of high-risk areas within the polygon from Sweco (2014), with a ratio of 23%.

<p align="center">*a*</p>

<p align="center">*b*</p>

<p align="center">*c*</p>
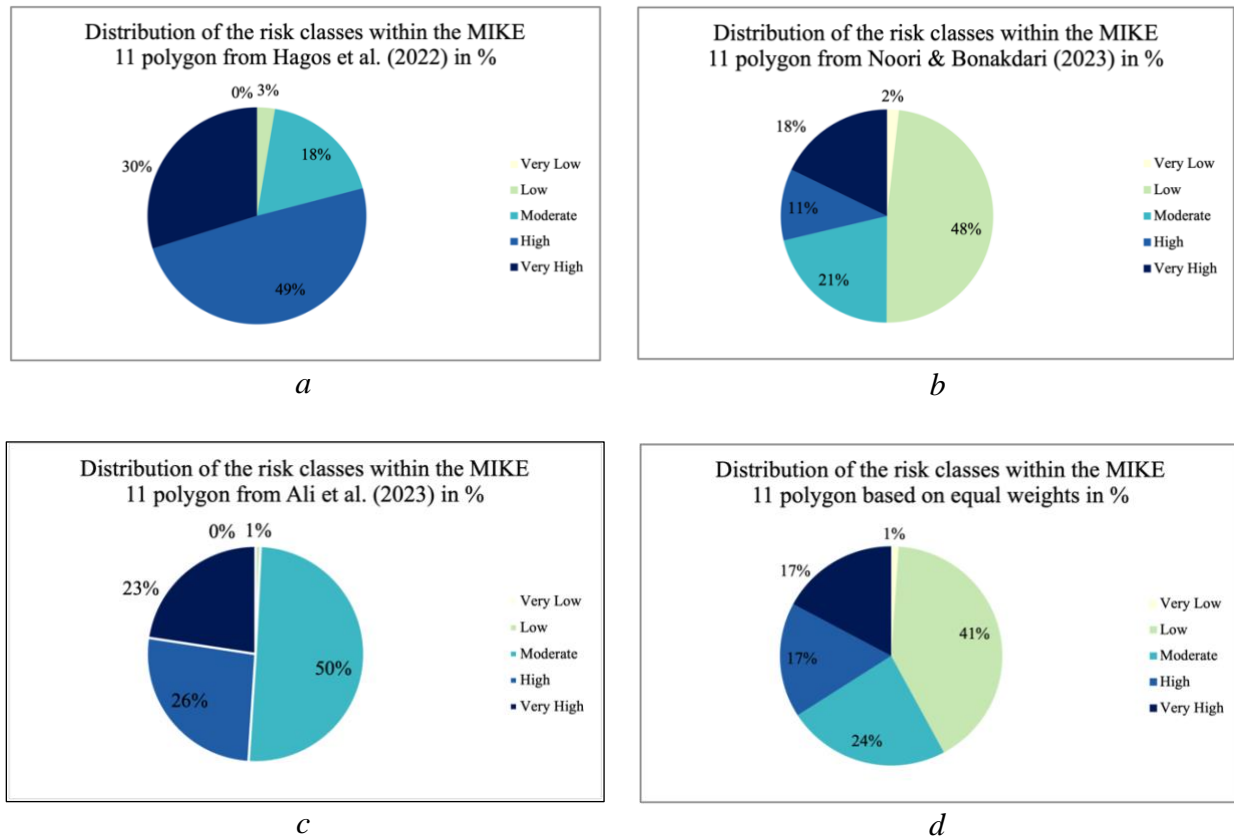

<p align="center">*d*</p>

Figure 14: Spatial distribution of the different risk classes in the polygon resulting from the MIKE 11 model. There are 4 results, one based on weights from Hagos et al. (2022) (a), Noori & Bonakdari (2023) (b), Ali et al. (2023) (c) and one based on equal weights(d).

4 Discussion

4.1 Interpretations on modelled flooding areas

This study on flood risk assessment in the Rönne å catchment used the GIS-based MCA method to identify flood-prone areas within the drainage basin (Ali. Et al. 2023). This involved analysing seven key parameters influencing flooding: elevation, soil, drainage density, slope, land cover, distance to the river, and monthly rainfall. Weighted coefficients from Ali et al. (2023), Noori & Bonakdari (2023) and Hagos et al. (2022) were used to establish the priority of these flood risk parameters. From that, four flood risk maps were created, and the risk was divided into 5 categories using the natural break approach, which also align with other papers such as Osman & Das (2023). This provided categorized flood risk maps ranging from very low to very high (figure 11). It is important to emphasize that the resulting flood risk maps illustrate the relative risk across the catchment area, rather than providing a precise measure of risk for any specific location. By analyzing figure 12, it was possible to conclude that the choice of the weights across the 7 factors had a moderate influence on the fraction of each of the risk classes across the catchment. However, the spatial distribution of those risk classes across the catchment was affected minimally by the chosen weights as illustrated in figure 11. The produced maps in figure 11 demonstrated that most of the high-risk classes were generally found in the in the north-west of the Rönne å river basin and was decreasing in the east and south. The cause of this might be due to the influence of elevation across the catchment as it is very low in those areas, as illustrated in figure 5. A second general pattern was recognized, where most of the high flood risk areas were close to the Rönne å river which confirms the hypothesis that areas close to rivers will be most affected. As this pattern is recognizable across all four flood-risk maps no matter the assigned weights of each factor, elevation might be the most significant factor for this catchment. When comparing the general high-risk areas from the four maps in figure 11 with the land cover and soil type maps in figure 8, it was evident that regions with high clay content soils and agricultural areas closely align with the very high-risk zones. This aligns with the expected results since agricultural areas are often rich in clay and clay soils with small particles often collect in valleys close to rivers where elevation is typically low (Hillel, 2008). The results of the flood maps from the MCA confirms the hypothesis that the most vulnerable areas prone to flooding are close to rivers (figure 11), as the Rönne å river is flowing in the west of the catchment from south to north (figure 1). When analyzing the general pattern of high-risk areas across the 4 flood risk maps in figure 11, areas close to rivers and with relatively low slope and elevation proved to be the most susceptible to flooding. This is consistent with the paper from Hagos et al. (2022) which assigned the highest weight to those factors. In addition, high risk areas close to the Rönne å river also tend to contain soils that are

rich in clay and are also agricultural areas. Since clay soils have low infiltration rates and agricultural areas are generally vulnerable to flooding, these factors enhance the high flood risk in those areas, which corresponds with the theory described earlier in the paper. Those areas are especially prone to high flood risk in Skåne, where a lot of natural wetlands have been drained in order to create more space for agricultural land, which could naturally be expected and agrees with other sources such as (Department of Environmental Conservation, 2024). Mitigation strategies could include reintroduction to natural wetlands in those areas as it helps slowing down water flow and increases the land's ability to retain water (Gabriels et al., 2022). Extreme precipitation events such as the Storm Hans in 2023 or the flooding event in the Ringsjön area in the south of the Rönne å catchment in January 2024 illustrated the extent of potential flooding scenarios which can be expected more frequently in the coming years due to climate change (Eklund et al., 2015). These predictions highlight the need for reliable flood risk maps and mitigation strategies not only in Sweden but across the world (United Nations Environment Programme, 2020). Therefore, it is crucial to analyze different flood modeling techniques and assess their reliability. In this paper, the MCA was chosen to compute flood maps that were compared to a flood map produced by Sweco (2014) which integrated a more complex hydraulic model MIKE11. The selection of MCA is justified by its efficiency in computation, ease of implementation, and reduced financial investment, making it advantageous for rapid and cost-effective flood risk assessments. In contrast, the MIKE11 model, while comprehensive, is not well-suited for extensive areas due to its complexity and the greater resources it requires for effective operation.

4.2 Comparing models

Before comparing 2 flood maps that were based on different approaches, it is crucial to understand what they are built upon and what outputs they have produced. As mentioned before, the flood risk map produced by Sweco (2014) utilized the MIKE11 hydrodynamic model, which is utilizing different approach when it comes to modeling flood risk in comparison to the MCA. While this method produced a flood risk map showing areas with different relative risk levels, MIKE 11 produced dynamic, time-based simulations of flood extends and depths, offering more precise flood predictions. After visually comparing the outputs from the MCA with the flood map from Sweco (2014), one can clearly see the different outputs that the 2 different approaches produced, with one showing general relative risk areas across the catchment and the other showing a detailed flood simulation map of a 200 – Year flow event shown in figure 14. Despite those different approaches, some similar patterns were observed. When analysing the high to very high-risk areas in the various produced maps against the MIKE 11 polygon (red outline) in figure 13, the map based on the weights from Hagos et al. (2022) demonstrated the best alignment with the MIKE 11 model (figure 13a). This conclusion was drawn by comparing the

dark blue areas (very high risk) with the red polygon outline. Since the red polygon simulates a flooding event, the flood risk in those areas is considered to be 100%. Therefore, the greater the overlap of the very high-risk areas from the MCA within this polygon, the more reliable the assessment. figure 14 further supports this observation, as the map based on Hagos et al. demonstrated the highest proportion of very high-risk areas within the red polygon, with 30% classified as very high risk and 49% as high risk. The reason the map based on the weights from Hagos et al. (2022) demonstrated better agreement with the map produced by Sweco (2014), might be due to the high importance assigned to slope and elevation. Since the Sweco map is based on MIKE 11, which also incorporates topography as a significant factor, this common emphasis on topographic features possibly explains their similarity compared to the other maps. The flood map produced based on the weights from Ali et al. (2023) showed the second-best correspondence with the red polygon, with 23% and 26% of the selected area classified as very high and high-risk areas, respectively. The map resulting from equal weights provided a low result which was to be expected since no factor in this analysis was put to the foreground. The map that showed the poorest performance in comparison to the red polygon layer was the one based on the weights from the article by Noori and Bonakdari (2023). The respective high and very high-risk areas within the polygon layer only covered 11% and 18%, respectively. This poor alignment might be due to the high weight assigned to the precipitation factor and the very low weights assigned to slope and elevation. As described in f7, the normalized values for precipitation have a very small spatial variation across the catchment, making the precipitation factor less relevant for determining distributed risk areas across Rönne å. The comparison between the flood map produced by Sweco (2014) and the maps resulting from the MCA concluded that, although the MCA covers the entire catchment area and identifies risk areas relative to the river basin, similarities to the more complex MIKE 11 model were observed. This indicates that the MCA can serve as an initial risk assessment tool to identify vulnerable areas. This paper demonstrated that the MCA has advantages, as it uses readily available data and employs a relatively simple methodology compared to other models. Therefore, it can be used as a preliminary study to assess flood risk zones over large areas.

4.3 Limitations and Future Research

4.3.1 Limitations

Although the MCA served as a general flood risk map, it incorporated various factors that require discussion due to the uncertainties and limitations they introduced into the resulting model.

4.3.1.1 Limitations of the factors used in the MCA

In the analysis of the elevation factor, it was assumed that all values above 100 meters had no flood risk and were assigned a normalized value of 0. This assumption was based on the catchment area, which varied between 0 and 227 meters, as shown in figure 5. However, it is unlikely that such a hard limit exists at 100 meters within the catchment where no flooding occurs. A more appropriate approach would have been to use elevation above drainage instead of elevation relative to sea level. This would have provided a more accurate representation of local water flow in relation to valleys and river networks. Additionally, it is important to note that the elevation factor was normalized specifically for this catchment area and cannot be generalized to other regions, as higher areas might experience different climates with more precipitation than lower-lying lands, altering the significance of this factor.

Similarly, the proximity to river factor was used to determine how distance to the river would influence flood risk. This was assessed using Euclidean distance, which calculates the distance to the river equally in all areas. However, this method does not accurately represent the natural flow of water and thus oversimplifies how the distance to the river influences the risk.

Furthermore, soil texture was correlated with its infiltration rate based on its clay, silt, or sand content, as well as coarseness and organic matter. However, the soil's infiltration rate also depends on additional factors such as soil structure, soil chemistry, and soil compaction. The arrangement of soil particles and their aggregation affect how easily water can infiltrate the soil. Well-structured soil allows for better water movement and less runoff. Soils rich in organic matter typically have improved infiltration due to better soil structure and porosity. Compacted soils have reduced pore spaces, which decreases infiltration rates (USAD & NRCS, 2014). These factors were not considered when using soil texture to determine infiltration rates. The choice of using the monthly precipitation data from August 2023, as shown in figure 7, was made to emphasize the importance of assessing flood risks, given that extreme precipitation events are becoming more frequent, thereby increasing flood risk. However, it would have been preferable to use a 30-year average of precipitation over the Rönne å catchment to generate a more representative precipitation pattern for the entire catchment. Given the catchment's size,

significant spatial variation in precipitation patterns is not expected, which limits the impact of choosing August 2023 on the overall results.

4.3.1.2 Important factors influencing flooding that were not considered

Pre-existing conditions prior to a flooding event are crucial as they significantly influence the extent of flooding. Continuous heavy rainfall can saturate the soil, reducing its ability to absorb additional water. This leads to increased water infiltration to the groundwater, raising the water table and potentially causing it to reach the surface, resulting in groundwater flooding. When the ground is frozen, it acts as an impermeable barrier, preventing water infiltration and causing surface runoff during rainfall or snowmelt. When the ground thaws, the accumulated water rapidly infiltrates, raising groundwater levels and potentially causing flooding source.

Pre-existing conditions affect groundwater levels and soil moisture content, which can either increase or decrease the extent of flooding. Dry soils have a higher capacity to absorb water, reducing surface runoff during rainfall and mitigating flooding. Conversely, wet soils or soils with high moisture content close to saturation have a reduced ability to absorb additional water. Before the extreme precipitation event in August 2023, there were periods of relatively dry months, with only July showing average precipitation. Therefore, it was assumed that soils prior to August were not saturated, and water infiltration was directly correlated to the varying infiltration rates of the soil textures. However, the response of soil moisture to precipitation can vary significantly over time and across different locations, often linked to seasonal changes in vegetation and climatic conditions. Another important factor that was not included in the MCA is the Topographic Wetness Index (TWI). TWI is a hydrological measure that quantifies the influence of topography on soil moisture and potential wet areas which is derived from digital elevation models (Kopecký et al., 2021). In an MCA for flood risk assessment, TWI is crucial as it helps identify saturated areas and potential flood zones. By integrating TWI with other factors, MCA can provide a more comprehensive flood risk map, highlighting areas with higher flood probabilities due to their topographic characteristics (Allende-Prieto et al., 2024).

4.3.2 Future studies

While this paper provides a useful initial approach for flood risk assessment using MCA and GIS, several improvements can be made. First, incorporating the factors discussed in the limitations section could optimize the MCA results. Considering pre-existing conditions before a flood event is crucial for a comprehensive understanding of the situation. Additionally, identifying the most influential factors affecting flooding in the Rönne å catchment area is essential. This could be achieved through expert surveys and fieldwork. Once the key factors are determined, enhancing the paper by developing a customized AHP, where the most relevant factors are given the highest weights, would provide a more accurate representation of real-world conditions compared to relying on weights from different articles. Incorporating a hydrological model, such as MIKE 11, into the MCA could significantly increase its accuracy. Finally, integrating socio-economic factors into the MCA would allow for assessing the vulnerability of areas affected by flooding, rather than merely quantifying regions at low or high flood risk.

5 Conclusion

To conclude, this paper used MCA together with GIS to do a flood risk assessment of the Rönne å catchment and used the following factors: Slope, Elevation, Drainage density, proximity to waterbodies, Soil types, Land cover and monthly precipitation. In this analysis, it was found that precipitation played the smallest role when talking about the spatial distribution of flood risk due to the small variation of the normalized values across the catchment. Slope and elevation were found to play crucial role when deciding on high and low risk areas across the catchment. Based on the MCA, most high-risk areas were found close to the Rönne å river and more in the northwest of the catchment. There were 4 flood maps produced based on different weights from Noori & Bonakdari (2023), Ali et al. (2023), and Hagos et al. (2022). It turned out the weights from Hagos et al. aligned best with the geographical and climatic conditions of the Rönne å catchment since it produced most high-risk areas within the polygon layer produced by Sweco (2014), which is simulating a flooding scenario.

6 References

Ali, Z., Dahri, N., Vanclooster, M., Mehmandoostkotlar, A., Labbaci, A., Zaied, M. B., & Ouessar, M. (2023). Hybrid Fuzzy AHP and frequency ratio methods for assessing flood susceptibility in Bayech Basin, southwestern Tunisia. Sustainability, 15(21), 15422. https://doi.org/10.3390/su152115422

Allende-Prieto, C., Roces-García, J., & Sañudo-Fontaneda, L. Á. (2024). The High-Resolution Calibration of the Topographic Wetness Index using PAZ satellite radar data to determine the optimal positions for the placement of Smart Sustainable Drainage Systems (SUDS) in urban environments. Sustainability, 16(2), 598. https://doi.org/10.3390/su16020598

Bennett, M. R., & Glasser, N. F. (Eds.). (2009). Glacial geology: Ice sheets and landforms (2nd ed.).
Beredskap. https://gisapp.msb.se/apps/oversvamningsportal/index.html

Bracken, L., Cox, N. J., & Shannon, J. P. (2007). The relationship between rainfall inputs and flood generation in south–east Spain. Hydrological Processes, 22(5), 683– 696. https://doi.org/10.1002/hyp.6641

Cabrera, J. S., & Lee, H. S. (2019). Flood-Prone area assessment using GIS-Based MultiCriteria analysis: a case study in Davao Oriental, Philippines. Water, (11), 2203. https://doi.org/10.3390/w11112203
California and Germany. *Frontiers in Environmental*

Cao, J., Yang, H., & Zhao, Y. (2021). Experimental analysis of infiltration process and hydraulic properties in soil and rock profile in the Taihang Mountains, North China. Water Supply, 22(2), 1691–1703. https://doi.org/10.2166/ws.2021.321
commun. https://www.engelholm.se/download/18.319a24a118cefac2cd52a96/1712754408
D., Olsson, J., Simonsson, L., & Sjökvist, E. (2015). Sveriges framtida klimat - Underlag till

Department of Environmental Conservation. (2024). Wetland Functions and Values: Water

Dragičević, N., Karleuša, B., & Ožanić, N. (2019). Different approaches to estimation of drainage density and their effect on the erosion potential method. Water, 11(3), 593. https://doi.org/10.3390/w11030593
Dricksvattenutredningen. SMHI Klimatologi Nr

Earth Networks. (2023, February 15). What is a Flood? - Earth Networks. Earth Networks . https://www.earthnetworks.com/flooding/#inland-flood

Eklund, A., Axén Mårtensson, J., Bergström, S., Björck, E., Dahné, J., Lindström, L., Nordborg,

Encyclopaedia Britannica. (2024). Talus | landform. https://www.britannica.com/science/taluslandform

EPA. (2023, November 2). Climate change indicators: Heavy precipitation. US EPA. https://www.epa.gov/climate-indicators/climate-change-indicators-heavyprecipitation

Erlström, M. (2009). Tectonic evolution and geological framework of Scania: A review of interpretations and geological models. SGU-report 2009:10.
Extension. https://extension.psu.edu/infiltrating-stormwater

Fransson, R., Persson, K. M., Leander, B., & Andersson, O. (January 2004). Saltwater distribution in the bedrock of Southwest Scania. In L. Araguás, E. Custodio, & M. Manzano

Gabriels, K., Willems, P., & Van Orshoven, J. (2022). A comparative flood damage and risk impact assessment of land use changes. Natural Hazards and Earth System Sciences, 22(2), 395–410. https://doi.org/10.5194/nhess-22-395-2022
GIS. Environment, Development and Sustainability, 25(3), 2316–

Hagos, Y. G., Andualem, T. G., Yibeltal, M., & Mengie, M. A. (2022). Flood hazard assessment and mapping using GIS integrated with multi-criteria decision analysis in upper Awash River basin, Ethiopia. Applied Water Science, 12(7). https://doi.org/10.1007/s13201-02201674-8

Hernández-Atencia, Y., Peña, L. E., Rojas, L. E. P., Rojas, I., & Alvarez-Rosario, A. (2023).

Hillel, D. (2008). 3. - SOIL FORMATION. In D. Hillel (Ed.), Soil in the Environment (pp. 177). Academic Press. https://doi.org/https://doi.org/10.1016/B978-0-12-348536-6.50008-3 http://www.geoglaciaire.net/images/documents/Matthew_Bennett;_Neil_F_Glasser_Glacial_geology.pdf https://resource.sgu.se/dokument/publikation/sgurapport/sgurapport200910rapport/s0910rapport.pdf https://www.smhi.se/data/ladda-ner-data/griddade-nederbord-och-temperaturdata-pthbv In www.naturvardsverket.se.

Inamdeen, F., Larson, M., Thiere, G. & Karlsson, C. (2021). LOCAL SCOUR IN RIVERS DUE TO BRIDGES AND NATURAL FEATURES. A CASE Investopedia. https://www.investopedia.com/terms/z/zscore.asp

IUCN. (2024). IUCN UK Peatland Programme. https://www.iucn-uk-peatlandprogramme.org/

Jarrett, A., & Emeritus. (2022). Infiltrating stormwater. PennState

Kaya, Ç. M., & Cengiz, L. D. (2023). Parameters and methods used in flood susceptibility mapping: a review. Journal of Water and Climate Change, 14(6), 1935–

Kopecký, M., Macek, M., & Wild, J. (2021). Topographic Wetness Index calculation guidelines based on measured soil moisture and plant species composition. Science of the Total Environment, 757, 143785. https://doi.org/10.1016/j.scitotenv.2020.143785

Kronvang, B., Larsen, S. E., Jensen, J. P., & Andersen, H. E. (2005). Catchment report: Rönne Å, Sweden. Trend Analysis, Retention and Source Apportionment. Norwegian Institute for

Krug, A. (1993). Drainage history and land use pattern of a Swedish river system - their importance for understanding nitrogen and phosphorus load. Hydrobiologia, 251(1–3), 285–

Kundtjänst. (2024, February 8). Januari 2024 - Höga flöden och översvämningar i Skåne. SMHI. https://www.smhi.se/klimat/klimatet-da-och-nu/manadens-vader-och-vattensverige/laget-i-sveriges-sjoar-och-vattendrag/januari-2024-hydrologi-1.203016 LibreTexts. https://geo.libretexts.org/Bookshelves/Geography_(Physical)/The_Physical_Environment_(Ritter)/11%3A_Soil_Systems/11.03%3A_Soil_Properties

Lidmar-Bergström, K., Elvhage, C., & Ringberg, B. (1991). Landforms in Skåne, South Sweden. Geografiska Annaler. Series A, Physical Geography, 73(2), 61–91. https://doi.org/10.2307/520984

Liu, J., Xu, Z., Chen, F., Chen, F., & Zhang, L. (2019). Flood hazard mapping and assessment on the Angkor World Heritage Site, Cambodia. Remote Sensing, 11(1),

Malczewski, J. (1999). GIS and multicriteria decision analysis. John Wiley & Sons.

Malczewski, J. (2006). GIS-based multicriteria decision analysis: a survey of the literature. International Journal of Geographical Information Science, 20(7), 703–726.

Mcleod, S. (2023). Z-Score: Definition, Formula, Calculation & Interpretation. Simply Psychology. https://www.simplypsychology.org/z-score.html#Interpretation

Messori, G., & Faranda, D. (2023, November 22). 2023/08/08 Storm Hans in Scandinavia. ClimaMeter. https://www.climameter.org/20230808-storm-hans

MSB. (2016). Översvämningsportalen. Myndigheten För Samhällsskydd Och

Nabati, J., Nezami, A., Neamatollahi, E., & Akbari, M. (2022). An integrated approach land suitability for agroecological zoning based on fuzzy inference system and Naturvårdsverket. https://www.naturvardsverket.se/4a43ca/contentassets/37e8b38528774982b5840554f02a1f81/produktbeskrivning-nmd-2018-basskikt-v2-2.pdf

Nevil, S. (2023, December 14). How to calculate Z-Score and its meaning.

NMD. (2020). Nationella marktäckedata 2018 basskikt: Produktbeskrivning.

NMD. (2018). National Land Cover Data 2018. Naturvårdsverkets Metadatakatalog FörGeodata.https://geodatakatalogen.naturvardsverket.se/geonetwork/srv/swe/catalog.search#/metadata/9c3310f6-73d5-4ae3-865f-0e16e03d44c8

Noori, A., & Bonakdari, H. (2023). A GIS-Based fuzzy Hierarchical Modeling for flood susceptibility Mapping: A case study in Ontario, eastern Canada. MDPI. https://doi.org/10.3390/ecws-7-14242

Nordström, S. (2024, April 2). Vattennivåer i Ringsjön och fakta om vattendomen + FAQ – Sydvatten. Sydvatten. https://sydvatten-se.translate.goog/vattennivaer-iringsjon/?_x_tr_sl=auto&_x_tr_tl=en&_x_tr_hl=de&_x_tr_pto=wapp

Opperman, J. J., Yarnell, S. M., Pawley, A., Shader, E., Cain, J., Zingraff-Hamed, A., Grantham, T. E., Eisenstein, W., & Schmitt, R. (2022). Restoring rivers and floodplains for habitat and flood risk reduction: Experiences in Multi-Benefit Floodplain Management from

Osman, S. A., & Das, J. (2023). GIS-based flood risk assessment using multi-criteria decision analysis of Shebelle River Basin in southern Somalia. SN Applied Sciences/SN Applied

Phillips, J. (2023, October 16). The soil texture triangle. AQUA-Research, ResearchGate, 77(3). https://www.researchgate.net/publication/355488600

Rincón, D., Khan, U. T., & Armenakis, C. (2018). Flood risk mapping using GIS and MultiCriteria Analysis: A Greater Toronto area case study. Geosciences, 8(8), 275. https://doi.org/10.3390/geosciences8080275

Ritter, M. (2022, February 19). 11.3: Soil properties. Geosciences Rönne Å Och Ringsjön. Ängelholm's

Saaty, T. L. (2008). Decision making with the analytic hierarchy process. International Journal of Services Sciences, 1(1), 83. https://doi.org/10.1504/ijssci.2008.017590

Schubert, P., 2004: Cultivation Potential in Hambantota District, Sri Lanka. Master Thesis in Physical Geography and Ecosystems Analysis, GIS Centre, Lund University. https://lup.lub.lu.se/luur/download?func=downloadFile&recordOId=1333068&fileOId=1333069

Science, *9*. https://doi.org/10.3389/fenvs.2021.778568

Sciences, 5(5). https://doi.org/10.1007/s42452-023-05360-5

Serra-Llobet, A., Jähnig, S. C., Geist, J., Kondolf, G. M., Damm, C., Scholz, M., Lund, J.,

SGU. (2023, May 2). Jordartsanalyser, öppna data. SGU Sveriges Geologiska Undersökning. https://www.sgu.se/produkter-och-tjanster/geologiska-data/oppnadata/jordarter-oppna-data/jordartsanalyser/

Shuaibu, A., Hounkpè, J., Bossa, Y. A., & Kalin, R. M. (2022). Flood risk assessment and mapping in the Hadejia River Basin, Nigeria, using hydro-geomorphic approach and multicriterion decision-making method. Water, 14(3709), 1-21. https://doi.org/10.3390/w14223709

SMHI. (2016). Ladda ner data från Svenskt

SMHI. (2024). SMHI. https://www.smhi.se/data/meteorologi/ladda-ner-meteorologiskaobservationer#param=airtemperatureInstant,stations=core,stationid=53530

SMHI. (2024, February 8). Januari 2024 - Höga flöden och översvämningar i Skåne. https://www.smhi.se/klimat/klimatet-da-och-nu/manadens-vader-och-vattensverige/laget-i-sveriges-sjoar-och-vattendrag/januari-2024-hydrologi-1.203016

SMHI. (2024). Nedladdning av griddad nederbörd- och temperaturdata (PTHBV).

Sofia, G., & Tarolli, P. (2017). Hydrological Response to ~30 years of Agricultural Surface Water Management. Land, 6(1), 3. https://doi.org/10.3390/land6010003

Storage   for   Flood   Water   and   Storm   Runoff.
STUDY FROM RÖNNE RIVER, SWEDEN LOKAL. Journal of Water Management and

Swedish Meteorological and Hydrological Institute. (2016). Vattendrag nätverk - SVAR2016.
https://www.smhi.se/data/utforskaren-oppna-data/vattendrag-natverk-svar2016

Tan, M., & Gullmander, E. (Project Managers). (2024). Slutrapport. In Projekt Destination

Thieken, A. H., Mohor, G. S., Kreibich, H., & Müller, M. (2022). Compound inland flood
events: different pathways, different impacts and different coping options. Natural Hazards
and Earth System Sciences (Print), 22(1), 165–185. https://doi.org/10.5194/nhess-22-
1652022

United Nations Environment Programme. (2020, March 3). How climate change is making
record-breaking floods the new normal. UNEP. https://www.unep.org/news-
andstories/story/how-climate-change-making-record-breaking-floods-new-normal

USAD & NRCS (2014). Soil infiltration. https://www.nrcs.usda.gov/sites/default/files/2022-
Use of Soil Infiltration Capacity and Stream Flow Velocity to Estimate Physical Flood

Van De Sande, B., Lansen, J., & Hoyng, C. (2012). Sensitivity of coastal flood risk assessments
to digital elevation models. Water, 4(3), 568–579. https://doi.org/10.3390/w4030568
Vattenarkiv.   https://www.smhi.se/data/hydrologi/sjoar-och-vattendrag/ladda-ner-data-
fransvenskt-vattenarkiv-1.20127
Vermont. https://dec.vermont.gov/watershed/wetlands/functions/storage#:~:text=By%20ho
lding%20back%20some%20of,as%20much%20as%2080%20percent.
Vulnerability   under   Land-Use   Change   Scenarios. Water, 15(6),
Water   Research   (NIVA).   https://niva.brage.unit.no/niva-
xmlui/bitstream/handle/11250/213016/5122_EH%20nr%2019.pdf?sequence=1
YIELD. https://www.aquayield.com/the-soil-texture-triangle

Zadeh,   L.   A.   (1965).   Fuzzy   sets. Information   and   Control, 8(3),   338–
Zhang, W., Hu, B., Liu, Y., Zhang, X., & Li, Z. (2023). Urban Flood Risk Assessment through
the Integration of Natural and Human Resilience Based on Machine Learning Models.
Remote Sensing, 15(14), 3678. https://doi.org/10.3390/rs15143678

7 Appendix

7.1 Soil and Rock types and their contribution to flooding

Table 7: Different soils that exist in the Rönne å catchment and their respective effect on flooding.

Soil and Rock types	Effect on flooding
Peat (Bog peat, Fen peat, Peat)	Peat soils are highly absorbent, capable of holding large quantities of water relative to their dry weight. This characteristic allows them to act like a sponge, absorbing precipitation and reducing immediate runoff, which can mitigate flood risks under normal conditions (IUCN, 2024).
Gyttja, Gyttja Clay	Organic-rich mud, gyttja often has a high silt and clay content, with gyttja clay being particularly rich in clay, which results in a low infiltration rate and thus presents high flood risk
Postglacial Sand, Aeolian Sand, Postglacial fine sand	These are predominantly sandy soils with coarse texture, characterized by large particle sizes and high drainage and thus presents low flood risk
Young Fluvial Sediment (sand, gravel), Glaciofluvial Sediment, Glaciofluvial Sand, Glaciofluvial Gravel	Fluvial and glaciofluvial deposits can vary but typically contain sand and gravel, indicating a coarser, well-draining texture indication low flood risk
Shingle, Talus (Scree)	Shingle and Talus have lower drainage rates due to the compact nature of the rock fragments and the potential for smaller particles to fill gaps between larger rocks, reducing permeability, indicating higher flood risk (Encyclopaedia Britannica, 2024)
Till, Gravelly Till, Sandy Till, Silty to fine sandy till	Till soils are a mix of materials deposited by glaciers, typically containing a mixture of clay, silt, sand, and gravel ❼ reduced flood risk
Rock, Sedimentary Rock, Crystalline Rock, Phanerozoic Dolerite	Rock types ❼ high flood risk

Table 8: Translated symbology from the soil layer obtained from SGU and their respective flood risk SGU (2018).

Soil type	Original Version	Effect on Flooding
Rock	Berg	high
Sedimentary rock	Sedimentärt berg	high
Crystalline rock	Urberg	high
Postglacial silt	Postglacial silt	low
Silt	Silt	low
Glacial silt	Glacial Silt	low
Sandy till	Vittringsjord, ler--silt	low
Silty to fine sandy till	Sandig-siltig morän	low
Young fluvial sediment, gravel	Svallsediment, grus	low - moderate
Shingle	Klapper	low - moderate
Glaciofluvial sediment	Isälvssediment	low - moderate
Glaciofluvial gravel	Isälvssediment, grus	low - moderate
Gravelly till	Grusig morän	low - moderate
Young fluvial sediment, gravel	Svämsediment, grus	low - moderate
Talus (scree)	Postglacial lera	low - moderate
Bog peat	Mossetorv	moderate
Fen peat	Kärrtorv	moderate
Gyttja	Gyttja	moderate
Till	Morän	moderate
Saprolite	Vittringsjord	moderate
Peat	Torv	moderate
Young fluvial sediment	Svämsediment	moderate
Gyttja clay (or clay gyttja)	Gyttjelera (eller lergyttja)	very high
Phanerozoic dolerite	Fanerozoisk diabas	very high
Glacial clay, clay content >25%	Svämsediment, ler--silt	very high
Glacial clay, clay content 15–25%	Postglacial grovlera	very high
Young fluvial sediment, clay to silt	Morängrovlera	very high
Postglacial clay, clay content >25%	Glacial lera	very high
Postglacial clay, clay content 15–25%	Sandig morän	very high
Clay till, clay content 15–25%	Sandig morän Talus (rasmassor)	very high
Saprolite, clay to silt	Vittringsjord, ler--silt	very high
Postglacial clay	Postglacial lera	very high

Till, clay content 5–15%	Lerig morän	very high
Postglacial sand	Postglacial sand	very low
Glaciofluvial sand	Isälvssediment, sand	very low
Young fluvial sediment, sand	Svämsediment, sand	very low
Postglacial fine sand	Postglacial finsand	very low
Clay till, clay content >25%	Postglacial grovsilt-finsand	very low
Glacial silt to fine sand	Glacial grovlera	very low
Postglacial coarse silt to fine sand	Postglacial finlera	very low
Glacial clay	Flygsand	very low
Aeolian sand	Sandig-siltig morän	very low
Water	Vatten	no data
Artificial fill	Fyllning	no data

7.2 Land cover classes and their contribution to flooding

Table 9: Translated symbology from the land cover layer obtained from NMD and their respective effect on flood risk NMD (2018).

Land cover	Land cover translation	Effect on flooding
Tallskog (pa vatmark)	Pine forest on wetland	Very low
Granskog (pa vatmark)	Spruce forest on wetland	Very low
Barrblandskog (pa vatmark)	Mixed coniferous on wetland	Very low
Lövblandad barrskog (pa vatmark)	Mixed forest on wetland	Very low
Triviallövskog (på våtmark)	Decidiuus forest on wetland	Very low
Ädellövskog (pa vatmark)	Deciduous hardwood forest on wetland	Very low
Triviallövskog med ädellövinslag (pa vatmark)	Deciduous forest with deciduous hardwood forest on wetland	Very low
Temporärt ej skog (pa vätmark)	Temporarily non forest on wetland	Very low

Oppen vätmark	Open wetland	Very Low
Tallskog (utanför vatmark)	Pine forest not on wetland	Low
Granskog (utanför vatmark)	Spruce forest not on wetland	Low
Barrblandskog (utanför vätmark)	Mixed coniferous not on wetland	Low
Lövblandad barrskog (utanför vatmark)	Mixed forest not on wetland	Low
Triviallövskog (utanför vatmark)	Decidiuus forest not on wetland	Low
Ädellövskog (utanför vätmark)	Deciduous hardwood forest not on wetland	Low
Triviallövskog med ädellövinslag (utanför vätmark)	Deciduous forest with deciduous hardwood forest not on wetland	Low
Övrig öppen mark utan vegetation	Non vegetated other open land	Moderate
Övrig öppen mark med vegetation	Vegetaded other open land	Moderate
Temporärt ej skog (utanför vatmark)	Temporarily non forest not on wetland	Moderate
Akermark	Arable land	High
Exploaterad mark, byggnad	Artificial sur- faces, building	Very high
Exploaterad mark, ej byggnad eller väg/järnväg	Artificial surfaces, building or road/railway	Very high
Exploaterad mark, vag/järnvag	Artificial surfaces, road/railway	Very high
Sjö och vattendrag	Inland water	no risk